PHILOSOPHICAL TRANSACTIONS OF THE ROYAL SOCIETY A MATHEMATICAL, PHYSICAL & ENGINEERING SCIENCES

Geophysical Evidence for the Locations, Shapes and Sizes, and Internal Structures of Magma Chambers beneath Regions of Quaternary Volcanism

H. M. Iyer

Phil. Trans. R. Soc. Lond. A 1984 **310**, 473-510
doi: 10.1098/rsta.1984.0005

Phil. Trans. R. Soc. Lond. A **310**, 473–510 (1984)
Printed in Great Britain

Geophysical evidence for the locations, shapes and sizes, and internal structures of magma chambers beneath regions of Quaternary volcanism

By H. M. Iyer
U.S. Geological Survey, 345 *Middlefield Road*, *Mail Stop* 77,
Menlo Park, *California* 94025, *U.S.A.*

This paper is a review of seismic, gravity, magnetic and electromagnetic techniques to detect and delineate magma chambers of a few cubic kilometres to several thousand cubic kilometres volume. A dramatic decrease in density and seismic velocity, and an increase in seismic attenuation and electrical conductivity occurs at the onset of partial melting in rocks. The geophysical techniques are based on detecting these differences in physical properties between solid and partially molten rock. Although seismic refraction techniques, with sophisticated instrumentation and analytical procedures, are routinely used for detailed studies of crustal structure in volcanic regions, their application for magma detection has been quite limited. In one study, in Yellowstone National Park, U.S.A., fan-shooting and time-term techniques have been used to detect an upper-crustal magma chamber. Attenuation and velocity changes in seismic waves from explosions and earthquakes diffracted around magma chambers are observed near some volcanoes in Kamchatka. Strong attenuation of shear waves from regional earthquakes, interpreted as a diffraction effect, has been used to model magma chambers in Alaska, Kamchatka, Iceland, and New Zealand. One of the most powerful techniques in modern seismology, the seismic reflection technique with vibrators, was used to confirm the existence of a strong reflector in the crust near Socorro, New Mexico, in the Rio Grande Rift. This reflector, discovered earlier from data from local earthquakes, is interpreted as a sill-like magma body. In the Kilauea volcano, Hawaii, mapping seismicity patterns in the upper crust has enabled the modelling of the complex magma conduits in the crust and upper mantle. On the other hand, in the Usu volcano, Japan, the magma conduits are delineated by zones of seismic quiescence. Three-dimensional modelling of laterally varying structures using teleseismic residuals is proving to be a very promising technique for detecting and delineating magma chambers with minimum horizontal and vertical dimensions of about 6 km. This technique has been used successfully to detect low-velocity anomalies, interpreted as magma bodies in the volume range 10^3–10^6 km^3, in several volcanic centres in the U.S.A. and in Mt Etna, Sicily. Velocity models developed using teleseismic residuals of the Cascades volcanoes of Oregon and California, and Kilauea volcano, Hawaii, do not show appreciable storage of magma in the crust. However, regional models imply that large volumes of parental magma may be present in the upper mantle of these regions. In some volcanic centres, teleseismic delays are accompanied by P-wave attenuation, and linear inversion of spectral data have enabled computation of three-dimensional Q-models for these areas. The use of gravity data for magma chamber studies is illustrated by a study in the Geysers-Clear Lake volcanic field in California, where a strong gravity low has been modelled as a low-density body in the upper crust. This body is approximately in the same location as the low-velocity body delineated with teleseismic delays, and is interpreted as a magma body. In Yellowstone National Park, magnetic field data have been used to map the depth to the Curie isotherm, and the results show that high temperatures may be present at shallow depths beneath the Yellowstone caldera. The main application of electrical techniques in magma-related studies has been to understand the deep structure of continental rifts. Electromagnetic studies in several rift zones of the world provide constraints on the thermal structure and magma storage beneath these regions.

1. Introduction

The generation, composition, and transport of magma, and shapes and sizes of magma chambers are of interest in understanding individual volcanic systems and major tectonic processes. In the past, geology and geochemistry have been the main tools used to study the evolution of volcanic systems. However, in recent years, geophysics has been making important contributions, mainly at the two ends of the spectrum of magmatic processes. At one end, geophysics is concerned with large-scale features such as, subduction zones, rift zones, collision boundaries, and crust and mantle beneath the plates themselves; and at the other end, it is concerned with small-scale phenomena associated with volcanic eruptions. Only recently are serious efforts being made to bridge the gap and to apply geophysical techniques to study the deep structure of individual volcanoes and volcanic systems.

This paper reviews the application of seismic and other geophysical techniques to detect and delineate magma chambers of a few cubic kilometres to several thousand cubic kilometres volume. The main emphasis will be on seismic techniques, mainly because of the large number of available case histories. The ideal way to present a review in the context of magma genesis would be to discuss case histories of a few well studied areas and to synthesize all available geophysical data. Unfortunately however, few such case histories are available, and therefore my plan will be to adopt a technique-oriented approach, emphasizing whenever possible, major results relevant to magma genesis in regions where a suite of geophysical techniques have been tried. My aim is to point out that techniques *are* now available to embark on the next phase of volcanological studies, namely, the use of a multi-disciplinary approach in several regions of the world, to address important questions on magma genesis.

1.1. *Magma chambers*

Geological evidence points to the existence of magma chambers in many different shapes and sizes. The magma in a chamber could be fully molten, partly molten, crystallized mush, or a combination of all these, and could range from basaltic to rhyolitic composition. The solidus temperature of rocks is in the range of 600–1300 °C with strong dependence on chemical composition, volatile content and pressure. Thus, the problem of studying magma chambers consists not only of estimating their shapes, sizes and depths, but also inferring their physical states and composition with measurable physical and chemical properties. Unique models of magma chambers, therefore, can be deduced only by a multi-disciplinary approach in which all available geological, geophysical, chemical and petrological tools are employed.

2. Geophysical techniques

Many geophysical tools are available for detecting magmatic systems. *Seismic* methods can be used to detect velocity and attenuation anomalies associated with magma. *Gravity* can reflect lateral variations in density of rocks caused by a zone of partial melting. Rocks cease to be ferromagnetic above the Curie temperature which is 560 °C for average crustal rocks and this property makes *magnetic* methods particularly useful for detecting magma. Resistivity of rocks depends on the proportion of melt in rocks, and *electrical* and *electromagnetic* methods use this property for detection of magma. I shall discuss these five methods, with emphasis on seismic methods.

3. Seismic techniques

Seismic techniques can be broadly divided into *active* techniques in which artificial sources such as explosions and vibrators are used to generate seismic waves and *passive* techniques in which earthquakes are used as the seismic sources. Previous reviews on the use of seismic techniques for magma chamber studies have been made by Piermattei & Adams (1973) and

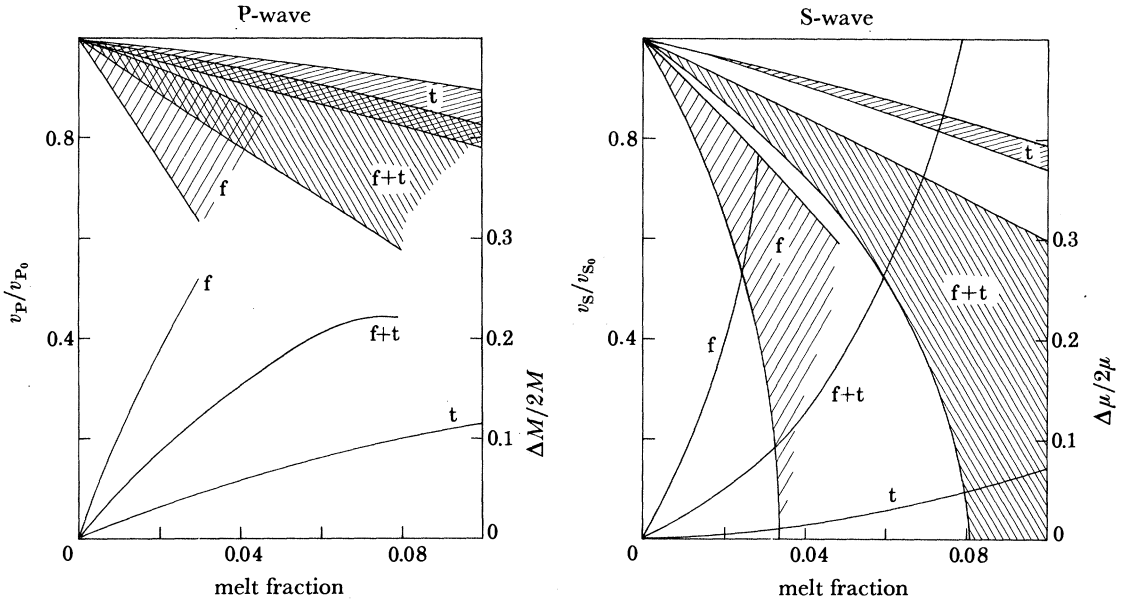

Figure 1. Computed P-wave and S-wave velocities and attenuation as a function of melt fraction for olivine at 20 kbar, 1600 K. (1 bar = 10^5 Pa.) v_P and v_S are velocities in partial melts and v_{P_0} and v_{S_0} are velocities in solid rock. $\Delta M/2M$ and $\Delta\mu/2\mu$ are respectively related P- and S-wave attenuation (Q^{-1}). Three different melt geometries are compared: t, tubes; f, films only; f+t, mixtures of tubes plus films where at any melt fractions 30% is in the form of films. The shaded regions show the range of dispersion (Mavko 1980). Copyright American Geophysical Union.

Sanford & Einarsson (1982). These techniques are based on the fact that P-wave and S-wave velocities in rocks decrease and attenuation increases at the onset of melting. Although the changes in velocities and attenuation depend on many factors, such as, composition and state of stress of the rock, fluid content, presence of cracks, and pore density and configuration in the rock, some general inferences on the state of melting can be made (Iyer & Stewart 1977). Few laboratory data are available on physical measurements in rock melts. Murase & McBirney (1973) showed that in some samples of basalt, andesite, and rhyolite, P-wave velocity decreased by a factor of 2 to 3 and P-wave attenuation increased by 2 to 3 orders of magnitude on transition from solidus to liquidus. Manghanani *et al.* (1981), using a continuous-wave interferometric method, obtained a velocity of 2.6 km s^{-1} and Q (reciprocal of attenuation factor) of about 20 in the melt of an alkaline basalt.

Owing to the paucity of laboratory data, the inferences on velocities and attenuation in rock melts are largely based on theoretical calculations with two phase systems (O'Connell & Budiansky 1974; Mavko 1980). Seismic-wave velocities decrease as the fluid inclusions in the rock matrix soften the rock mechanically. The time-dependent processes caused by the melt, such as viscous flow, result in wave attenuation. The extent of the calculated variations depend upon the melt geometries and relaxation models assumed. Mavko prefers melt geometry in the

form of tubes rather than films and spheres assumed in earlier calculations. Figure 1 shows Mavko's results for a typical mantle rock (olivine) for tubular and other melt geometries.

The wide dispersion in the results is quite obvious. For example, for 5% partial melt, P-wave velocity can decrease by a factor of 0.1–0.4, S-wave velocity by a factor of 0.1–1, and P and S attenuation by a factor of 1–3. These results highlight the difficulties associated with interpreting seismic observations and only qualitative interpretations of velocity and attenuation anomalies can therefore be given. More laboratory data on a variety of rock specimens as a function of temperature and pressure are needed to proceed from the detection and delineation stage to a quantitative understanding of magma genesis.

4. Active seismic techniques

Even though active seismic techniques are used extensively in oil exploration and are the basic research tools employed to infer the detailed structure of the Earth's crust and upper mantle, their application to the study of magma chambers has been very limited. In this section, I shall discuss the few cases in which seismic refraction, fan-shooting, and reflection techniques have been used for the study of magma chambers.

4.1. *Seismic refraction*

Detailed seismic refraction studies in the U.S.A., Hawaii (Hill 1969; Zucca *et al.* 1982), Yellowstone National Park–Eastern Snake River Plain (Smith *et al.* 1982), and Imperial Valley (Fuis *et al.* 1982), provide examples of the use of seismic refraction to explore the deep structure of volcanic regions.

To illustrate how the seismic refraction technique, if properly used, can be a powerful tool

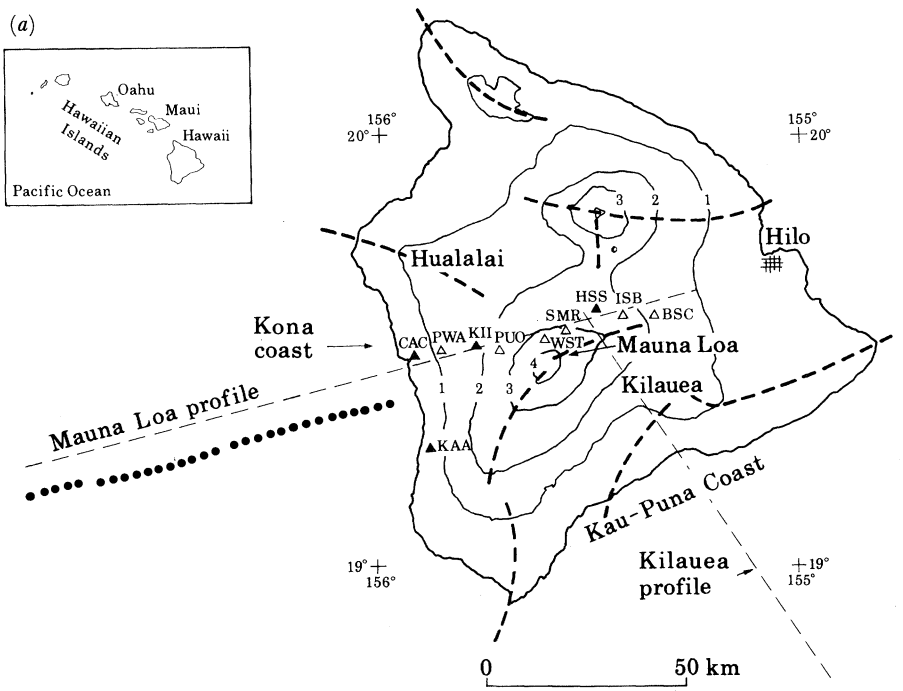

FIGURE 2*a*. For description see opposite.

to detect and delineate magma chambers, a study by Zucca *et al.* (1982) of the Mauna Loa volcano, Hawaii, is presented. In this study, though no magma chambers were located explicitly, a detailed crustal structure of the volcano was obtained. Thirty evenly spaced shots were set off perpendicular to the Kona Coast in the Island of Hawaii (figure 2*a*) and were

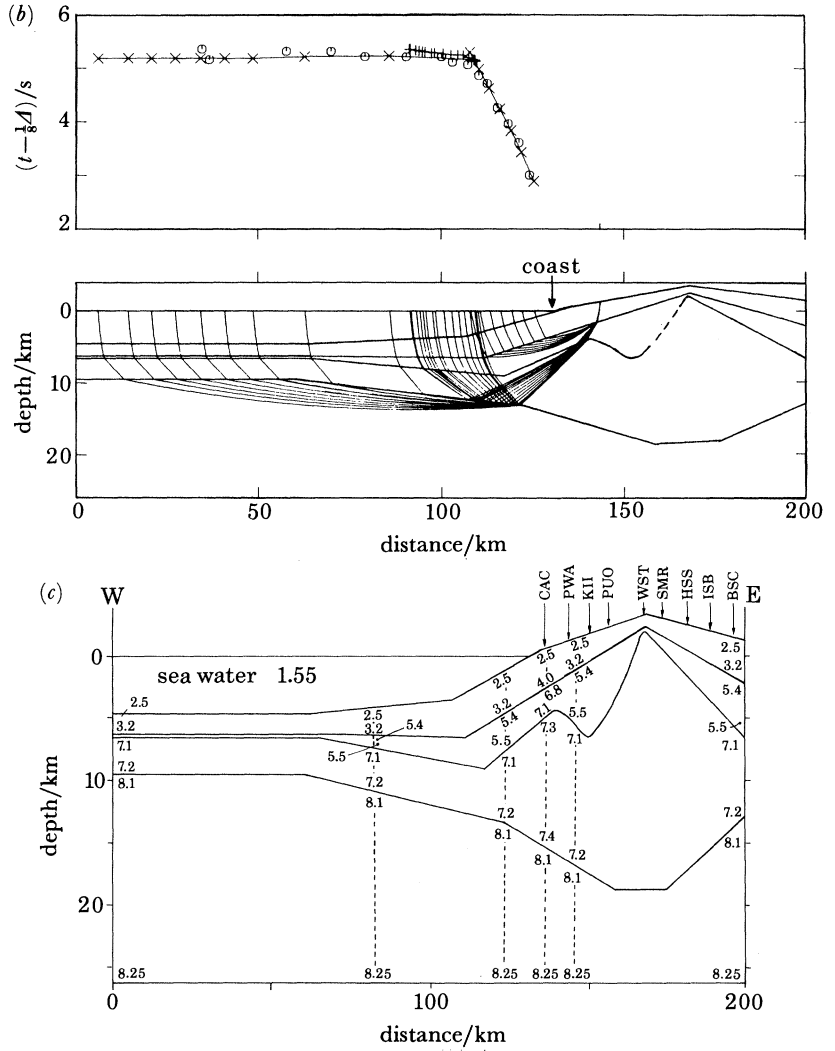

FIGURE 2. Seismic refraction study of the Mauna Loa volcano, Hawaii. (*a*) Dots are shot locations; triangles are seismograph stations; light dashed lines are gravity profiles; closed contours are elevation (contour interval 1 km); heavy dashed lines show rift zones. (*b*) Ray diagrams from shots to station PWA. Upper curve shows reduced travel time where t is travel time in seconds; distance Δ is in kilometres; reducing velocity is 8 km s^{-1}. Open circles are observed travel times and crosses are computed travel times. (*c*) Velocity structure using data from station PWA. Vertical exaggeration 4:1. Velocities are for compressional waves in km s^{-1} (Zucca *et al.* 1982). Copyright American Geophysical Union.

recorded by a linear array of inland stations providing a 100-km-long refraction profile. The seismic data were used to model the crust as follows. A starting model for the southeast coast of Hawaii based on earlier work was systematically changed until theoretical travel times computed by using a ray-tracing program agreed with the observed travel times to within 0.1 s. Figure 2*b* shows the rayplots to station PWA, and figure 2*c* shows the final model. The main features of the model are the high velocity oceanic layer (layer 3) in the crust and land-

ward dipping Moho. Zucca *et al.* modelled the fine structure of the crust–upper mantle transition zone with amplitude data and synthetic-seismograms, supplemented by gravity data. They concluded that Hawaii is composed of a pile of massive volcanic flows the weight of which has caused the lithosphere to be depressed by about 9 km. No magma chambers were detected though Koyanagi *et al.* (1975) had postulated the presence of a magma chamber under Mauna Loa based on the paucity of earthquakes in the depth range of 15–30 km.

4.2. *Fan shooting*

In this technique, shots and seismic arrays are positioned on opposite sides of the anomaly under investigation, to look for a 'shadow'. Schilly *et al.* (1982) present a very clear instance of detection of an upper-crustal magma body in the Yellowstone caldera by using fan-shooting. The study was part of a detailed seismic refraction experiment in the Snake River Plain–Yellowstone volcanic sub-province, U.S.A. (Smith *et al.* 1982). Previous studies have shown that the Yellowstone caldera is underlain by a large magma chamber probably extending from the crust into the upper mantle (see §5.5.1). Shot and instrument locations of the fan-shooting experiment and the seismograms plotted by azimuth with a reducing velocity of 5.95 km s^{-1} are shown in figure 3*a*. The large delays, reaching a maximum of 1.5 s seen in the azimuth range of 200–230° in the fan plot, are interpreted to be caused by a low-velocity body in the depth range of 3–9 km under the Sour Creek resurgent dome inside the Yellowstone caldera. The lateral extent of the body could be varied from 10–30 km depending on the choice of a velocity contrast from 30–10 %.

In another analysis of the Yellowstone refraction data, Lehman *et al.* (1982) applied a delay-time analysis to the P_g arrivals traversing the crystalline basement, to determine the three-dimensional distribution of velocities and layer configuration of the upper crust beneath the caldera (figure 3*b*). They detected low-velocity bodies under the Sour Creek and the Mallard Lake resurgent domes. By using additional constraints from gravity data, they found that the northeastern (Sour Creek) velocity anomaly was associated with a density decrease, whereas, the southwestern anomaly (Mallard Lake) was not. The Sour Creek dome anomaly with a compressional wave velocity decrease of 30 % and density decrease of 9 % was interpreted as partly molten rock and the Mallard Lake anomaly was interpreted as a fluid-filled fracture zone.

4.3. *Magma chambers in oceanic rifts*

In recent years there has been rapid advancement in the study of oceanic rifts from using sophisticated multi-channel seismic surveys. The focus of these studies has mainly been in the mid-Atlantic Ridge (M.A.R.) and the East Pacific Rise (E.P.R.). Several reviews on this subject are available (Fowler 1976, 1978; Nisbet & Fowler 1978; Sanford & Einarsson 1982; Edmond 1983; Macdonald 1983).

There is growing evidence for the presence of axial magma chambers beneath several sections of the fast-spreading (opening rate 5–18 cm a^{-1}) E.P.R. With travel-time delays and amplitude variations observed in seismic refraction data, low-velocity zones interpreted as shallow crustal magma chambers have been found under the spreading axis at 9° N, 12° N, 13° N, 15° N, 21° N, 22° N, and 10° S of the E.P.R. (Macdonald 1983). However, refraction and reflection studies of the slower spreading (2.9 cm a^{-1}) Juan de Fuca Ridge do not show the presence of a crustal magma chamber. The seismic technique used in these studies is best illustrated by the work done by three different groups in the 9° N section of the E.P.R. in the

PHILOSOPHICAL TRANSACTIONS OF THE ROYAL SOCIETY A MATHEMATICAL, PHYSICAL & ENGINEERING SCIENCES

PHILOSOPHICAL TRANSACTIONS OF THE ROYAL SOCIETY A MATHEMATICAL, PHYSICAL & ENGINEERING SCIENCES

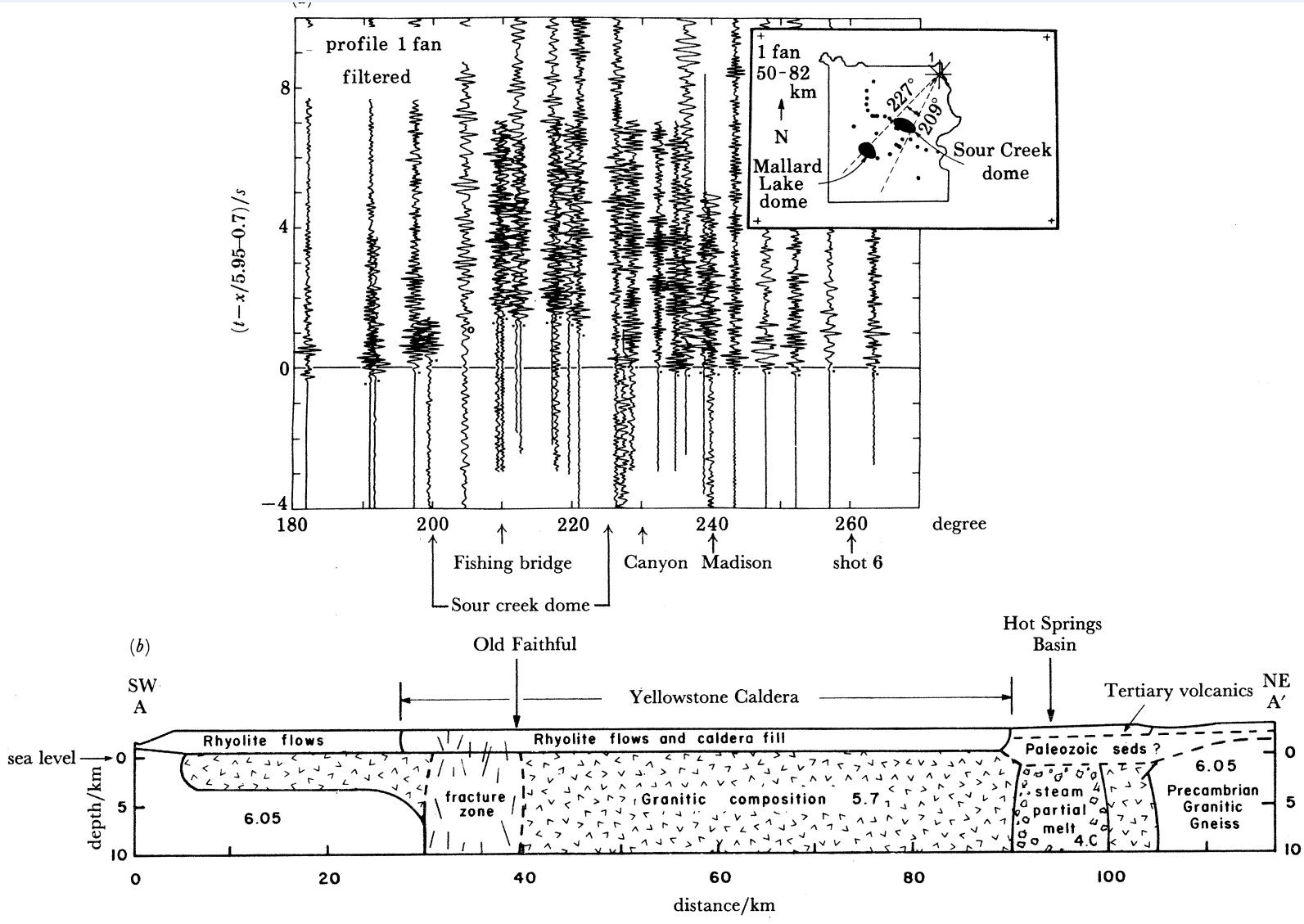

FIGURE 3. Seismic refraction experiment in Yellowstone National Park, Wyoming, U.S.A. (*a*) Seismic record section plotted in an azimuthal fan, reduced travel time against azimuth; t is the travel time in seconds, x is the distance in kilometres, reducing velocity is 5.95 km s^{-1}. Data correspond to distance ranges of 50–82 km. Insert shows Yellowstone National Park boundary, location of the resurgent domes, shot and station locations, and azimuthal window over which anomalous delays are observed (Schilly *et al.* 1982). Copyright American Geophysical Union. (*b*) Geologic cross section through the upper crust of Yellowstone caldera based on delay-time analysis of seismic refraction data and gravity modelling. Numbers are P-wave velocities in km s^{-1} (Lehman *et al.* 1982). Copyright American Geophysical Union.

vicinity of the Siqueiros Fracture zone. Orcutt *et al.* (1976) shot three parallel profiles, along the ridge crest, parallel to the crest axis on 2.9 Ma old crust, and on 5 Ma old crust. A low-velocity zone, 1.4 km thick and 2 km deep, was found under the ridge crest. The mantle velocity was lower under the ridge crest and progressively increased with age on the other profiles. The low-velocity zone was interpreted as partly molten rock. Rosendahl (1976) and Rosendahl *et al.* (1976) shot 21 refraction profiles in the same area of the E.P.R. Their preferred model shows a wedge-shaped crustal low-velocity zone under the axis of the rift which tapers to zero thickness at the margins of the axial block. This body is interpreted to contain 30% partial melt. Herron *et al.* (1978) used seismic reflection profiling and identified what appears to be the top of this magma chamber. By re-migrating reflection data with detailed velocity information from laboratory measurements of ophiolite samples, Hale *et al.* (1982) have produced a sharply focused boundary for this magma body. This reflection boundary which is one-sided, indicates a magma chamber with an upward slope of about 10° towards the ridge crest and a half width of 4 km from the ridge axis.

In contrast, seismic refraction studies in the M.A.R. have failed to find crustal magma chambers, although there is strong evidence for a low-velocity zone in the mantle beneath the ridge axis. There has been special focus in two regions of the M.A.R., near 37° N (FAMOUS area) and 45° N. The absence of shallow crustal magma chambers beneath the slow-spreading (1.9–2.3 cm a^{-1}) M.A.R. and their presence in the fast-spreading E.P.R. has led to speculations on the origin of magma chambers in oceanic ridges. Pending resolution of this question, an acceptable model for the M.A.R. is that proposed by Nisbet & Fowler (1978). In this model, magma generation and accumulation occur at sub-crustal depths, with the magma injection into the crust and ridge itself taking place by vertical crack propagation or by the development of long, narrow, magma conduits.

4.4. *Time delays, and attenuation caused by diffraction*

Magma bodies have been located in Kamchatka, U.S.S.R., by using active and passive seismic techniques. These studies include: (*a*) structure of small magma bodies associated with eruptions; (*b*) location of upper-crustal resident magma bodies; (*c*) parental magma sources in the lower crust and mantle; and (*d*) regional structure of the crust and upper mantle. The Russian techniques consist of measuring P-wave delays, P-wave attenuation, and shadow effects caused by diffraction.

A typical active experiment is described by Utnasin *et al.* (1976) in the Klyuchevskoy group of volcanoes (figure 4).

Refraction and deep reflection data were first used to establish a control model for the region along profile I–I′ in an 'amagmatic' zone. Along profile II–II′ reflected seismic waves from shots 1, 3, and 4, showed anomalous apparent velocities owing to refraction, attenuation, and travel-time offsets, presumably caused by strong lateral inhomogeneities. These phenomena were modelled assuming diffraction around a low-velocity body, 10 km long, 5 km wide, with its top at a depth of 10 km under the Bezymyanny volcano. The P-wave velocity inside the body was estimated to be 5.3 km s^{-1} in comparison with a normal velocity of 6.6 km s^{-1} in the surrounding rock. In order to derive the deeper structure of the volcanic group, a fan-shooting profile was deployed by using shot 3 and profiles I′–II′. A similar body was located under the Kamen volcano and a long magma conduit was recognized under the Klyuchevskoy volcano extending from the crust to the mantle and connected to a large magma zone in the

PHILOSOPHICAL TRANSACTIONS OF THE ROYAL SOCIETY A MATHEMATICAL, PHYSICAL & ENGINEERING SCIENCES

PHILOSOPHICAL TRANSACTIONS OF THE ROYAL SOCIETY A MATHEMATICAL, PHYSICAL & ENGINEERING SCIENCES

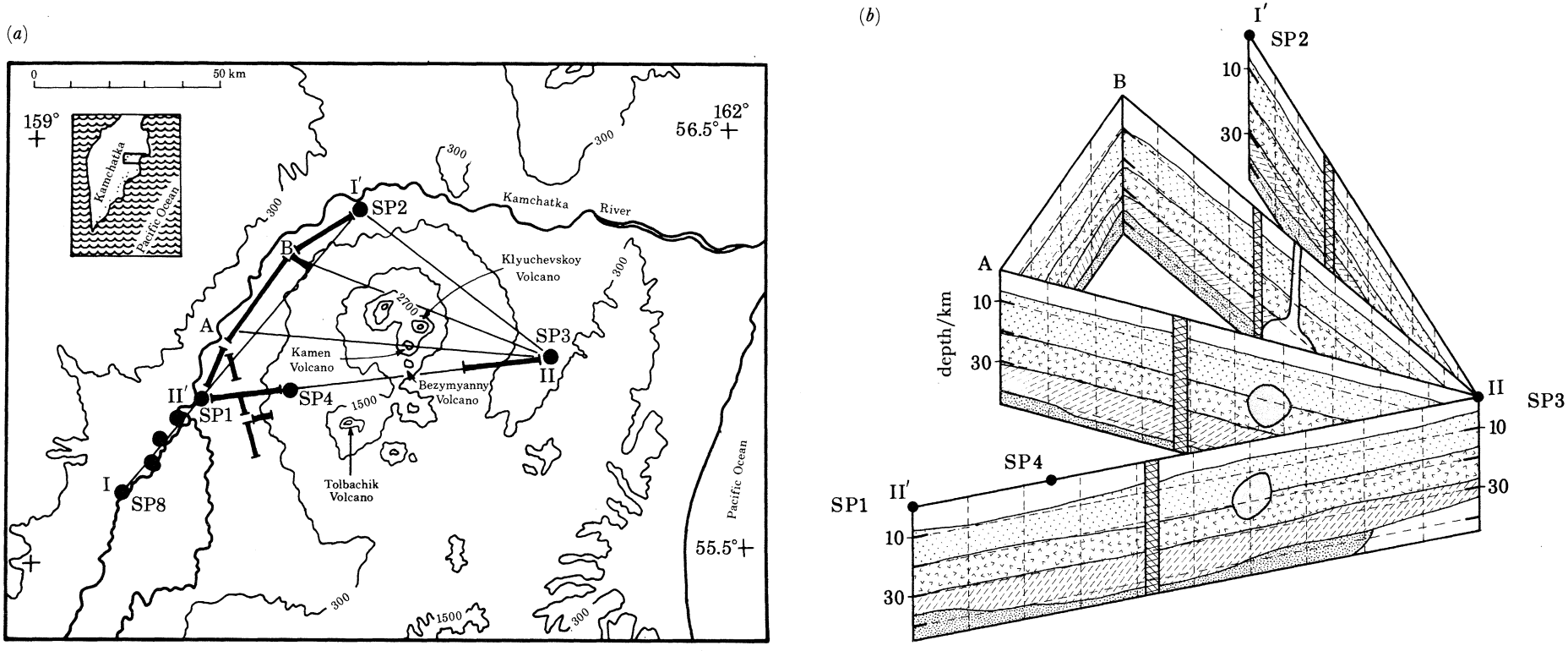

FIGURE 4. Active seismic experiment in the Kamchatka volcanoes, U.S.S.R. (*a*) Scheme of seismic experiment (see insert for location). SP1, SP2, SP3, SP4 are shot points; solid lines are seismic profiles. (*b*) Fence diagram of seismic cross sections along dark lines in (*a*). Magma chambers are shown by irregular circles. The vertical and horizontal seismic boundaries are approximate. Figure is adapted from Utnasin *et al.* (1976). Copyright Tokai University Press.

upper mantle (figure 4*b*). The authors speculate that a probable model for the Kamchatka volcanoes consists of small chambers and conduits in the crust, and secondary chambers and a deep-seated parental magma source in the upper mantle.

Balesta *et al.* (1978) used several fan shooting profiles to locate magma chambers under the newly formed (during 1975–6) Tolbachik volcanoes (figure 4*a*). Seismograms from the profiles showed shadow zones characterized by wave-amplitude oscillations at the shadow boundary, frequency decrease within the shadow zone, and emergence of a 'small wave' in the central part of the zone. These were interpreted as diffraction effects caused by an obstacle with lower-than-normal visco-elastic parameters. Several small magma bodies with diameters of about 3 km were identified in the region.

Balesta & Farberov (1968) used longitudinal and fan-shooting profiles in the Piip crater, which formed in October 1966 on the northern flank of the Klyuchevskoy group of volcanoes, and identified regions of strong P-wave attenuation and delays. These were modelled as pockets of magma with a horizontal size of 100 m × 40 m. The authors also measured compressional wave velocity in an incandescent lava dome and found it to be 750–800 m s^{-1} and, from seismic attenuation, estimated a viscosity of 0.6×10^{10} P.†

4.5. *Reflection*

One of the most powerful techniques in modern seismology, primarily developed for oil exploration but now being recognized as a very effective tool for detailed imaging of the lithosphere, is seismic reflection using Vibroseis‡. Use of this technique in the Socorro, New Mexico, region of the Rio Grande Rift, U.S.A., has given some remarkable results (Brown *et al.* 1980). A magma chamber has been postulated to exist in the upper crust in this region from study of reflected shear waves in seismograms of local earthquakes (Sanford *et al.* 1973, 1977) (see §5.3). The location of the profiles and line drawings of the prominent reflections are shown in figure 5. Note the high amplitude reflections seen between 6 and 8 s, corresponding to depths of 18–25 km. Brown *et al.* make several inferences on the reflector. The lack of pronounced reflection from the bottom of the anomaly indicates that either the base of the anomalous body is not a good reflector or the body is thin, and probably sill-like. The body, though horizontally having a large area, is limited in extent. On the east it seems to end as a high amplitude event, and on the west it seems to splay into several branches. On line 2A it was found to diffuse in the north and south ends. Based on shear-wave reflection data, heat flow, and contemporary volcanism, and uplift in the Socorro area, the reflector was inferred to be a magma body.

Brocher (1981) computed reflectivities by using the data to infer the physical nature of the Socorro magma intrusion. Reflectivity is the ratio of the spectra of the reflected and the incident waves. Brocher compared observed reflectivities with reflectivities of theoretical models of plane-parallel-layered magma intrusions, 35–38 m thick, with velocities of 3.5–3.8 km s^{-1} (velocity in crustal rocks 6.0 km s^{-1}). Other models, such as a series of horizontally discrete pods, and a continuous body having a periodic curvature on the scale of the wavelength of the incident wave, were also tried. The best fitting models were those with several layered magma intrusions. Modelling of the reflectivity therefore suggests that the Socorro magma body is a multi-layered intrusive complex.

In one of the few other documented cases of reflection from a hypothetical magma chamber,

† 1 P = 10^{-1} Pa s.
‡ Trade mark Continental Oil Company.

PHILOSOPHICAL TRANSACTIONS OF THE ROYAL SOCIETY A MATHEMATICAL, PHYSICAL & ENGINEERING SCIENCES

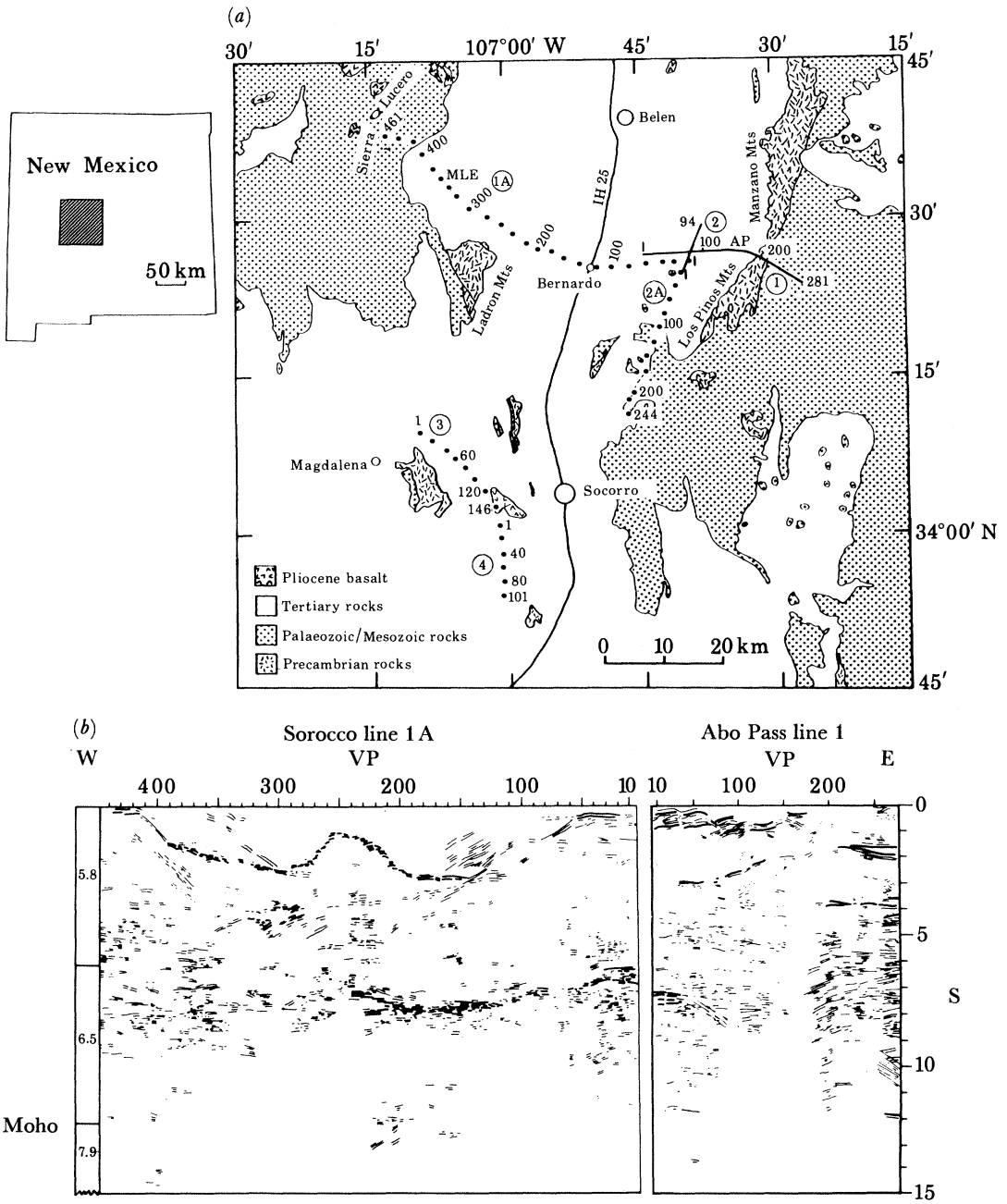

FIGURE 5. Seismic reflection studies in the Rio Grande Rift. (*a*) Location of COCORP seismic reflection lines in the Socorro region of the Rio Grande rift, New Mexico. Line numbers are circled and vibrator locations (VP) (dots) labelled. MLE is Monte Largo Embayment, AP is Abo Pass. (*b*) Line drawing emphasizing prominent features on the seismic sections from lines 1 and 1A. On the left is shown the crustal velocity section from available seismic refraction data (Brown *et al.* 1980). Copyright American Geophysical Union.

Hill (1976) reported late arrivals in refraction seismograms in the Long Valley caldera, California, which could be interpreted to have bounced off the roof of a magma chamber. Geologic evidence suggests the existence of a magma chamber in this area and Steeples & Iyer (1976), with use of teleseismic P-wave residuals (see §5.5.3), confirm its existence at depths of approximately 5–25 km under the caldera.

5. Passive seismic techniques

Several published case histories are available, on detection and delineation of magma chambers, which use passive seismic techniques. Patterns of seismicity around volcanoes, attenuation of seismic body waves (particularly S-waves), reflected phases from earthquakes, and delays in teleseismic waves as they propagate through anomalous material under volcanoes have all been used to detect magma chambers in the crust and mantle.

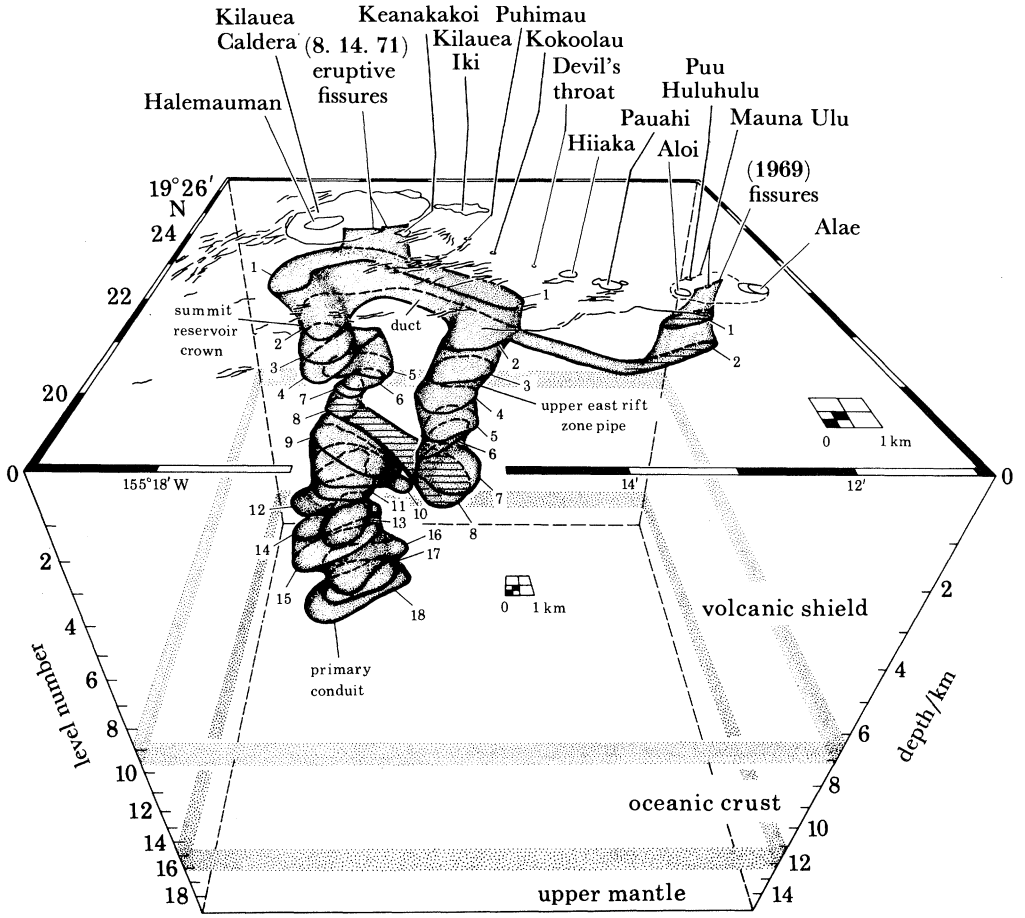

Figure 6. Three-dimensional perspective construction of magma conduits in Kilauea volcano, Hawaii, with seismicity data. The view is looking north into the interior of the volcano. Numbers (1–18) correspond to level numbers within the model (Ryan *et al.* 1981). Copyright American Geophysical Union.

5.1. *Mapping magma conduits with seismicity*

Seismicity beneath volcanoes is caused by magma-induced and tectonic stresses. If zones of partial melt are present, earthquake stresses cannot accumulate within them, though the pressure exerted by the magma is responsible for the seismic activity in surrounding rock. Zones of seismic quiescence may therefore indicate the locations of magma chambers. Such zones have been found at depths of 20–200 km beneath some of the Kamchatka volcanoes in the U.S.S.R. (Farberov *et al.* 1973, 1979). Since strong attenuation of S-waves also seems to occur in these aseismic zones (see §5.2), they have been interpreted as regions of low viscosity

associated with magma. Locations of microearthquakes associated with the eruptions of Usu volcano in Japan has been used by Okada *et al.* (1981) to infer the zone of magma intrusion. The hypocentres were located in a narrow cylindrical volume enclosing an earthquake free zone, interpreted as the zone of magma intrusion to the top of the volcano.

Seismicity patterns beneath Kilauea volcano, Hawaii, were used by Koyanagi *et al.* (1976) and Ryan *et al.* (1981) to map magma conduits. Detailed seismic refraction studies (Hill 1969) and teleseismic studies (Ellsworth & Koyanagi 1977) have shown that no large magma chambers exist in the crust under Kilauea. Duffield *et al.* (1982) suggest that the magma in Hawaii is transported from the mantle to a secondary reservoir located 2–6 km beneath the summit of the volcano from where it erupts to the summit caldera and rift zones. Ryan *et al.* (1981) stacked horizontal, two-dimensional sections of the seismicity plots to infer the three-dimensional pattern. The horizontal sections were made on clear plexiglass so that the final volume could be observed from any vantage point to make inferences on the shapes of interesting features of the seismicity pattern. In the final interpretations, magma conduits were defined as zones of seismicity, not zones of seismic 'quietness'. The magma transport passageways were visualized as honeycomb-like, magma-filled, fracture zones. The lateral extent of seismic hypocentres, within the standard errors of their locations, define the conduits. Figure 6 shows a three-dimensional perspective construction. The primary magma conduit can be traced to a depth of 14.6 km in the upper mantle and rises through the crust into the volcano edifice, where the structure of the conduits become very complex leading to the volcanic crown and the east rift zone.

The zone of intense seismic activity preceding the violent eruption of Mount St Helens, U.S.A. in 1980 may also be indicating a zone of fracturing caused by the presence of magma in the upper crust. About 700 earthquakes were precisely located from March 20 to the date of the catastrophic eruption, May 18, 1980. All the earthquakes were confined to a small volume in the depth range of 1–6 km in a region directly beneath the zone of intense deformation (Endo *et al.* 1981).

5.2. *Seismic wave attenuation*

The first determination of the depth of a magma chamber by using seismic techniques was made by Gorshkov (1958) in the Klyuchevskoy group of volcanoes in Kamchatka. He found that in the seismograms of some earthquakes with epicentres in southern Japan recorded by the Kamchatka seismic station Kliuchi, longitudinal waves were clear, but transverse waves were absent. Earthquakes from the same azimuth but at greater distances (meaning steeper incident waves at the station), and from different azimuths, showed distinct S-arrivals on the seismograms. Gorshkov proposed that the S-wave absorption was caused by the presence of a magma reservoir under the Klyuchevskoy volcano. He estimated the depth of the magma zone to be between 50 and 70 km under the volcano. From the extent of the shadow boundaries, he inferred the shape of the reservoir to be a convex lens or a triaxial ellipsoid with a thickness of 25–35 km. Even though the data were quite marginal, Gorshkov calculated the velocity in the magma reservoir to be 1.6–1.8 km s^{-1}. Gorshkov found no evidence for the existence of shallow magma chambers.

Anomalous attenuation of S-waves from local and regional earthquakes has also been observed in the region of the Avacha–Koryasky group of volcanoes (Farberov & Gorelchik 1971; Farberov *et al.* 1973). The ratio of the maximum amplitude and maximum period (A/T) of SH-waves at five stations were compared with corresponding ratios at a reference

PHILOSOPHICAL TRANSACTIONS OF THE ROYAL SOCIETY A MATHEMATICAL, PHYSICAL & ENGINEERING SCIENCES

station Petropavlosk (PTR). The ratios $(A/T)_{\mathrm{I}}/(A/T)_{\mathrm{PTR}}$, where I is the station name, when plotted as a function of event azimuths, were found to fluctuate with discrete maxima and minima (figure 7), the minima corresponding to the azimuths from the stations to the volcanoes. Attributing the fluctuations of (A/T) to diffraction, Farberov & Gorelchik, with simple diffraction theory, computed the cross sections of the causative bodies to be 8–30 km and their depths 30–100 km.

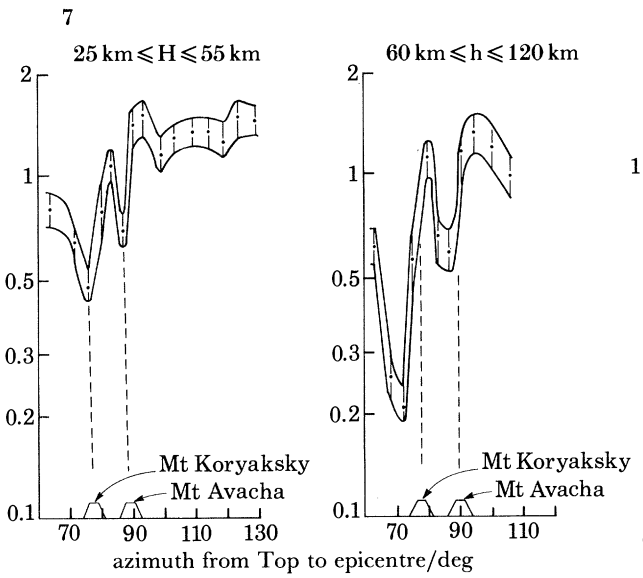

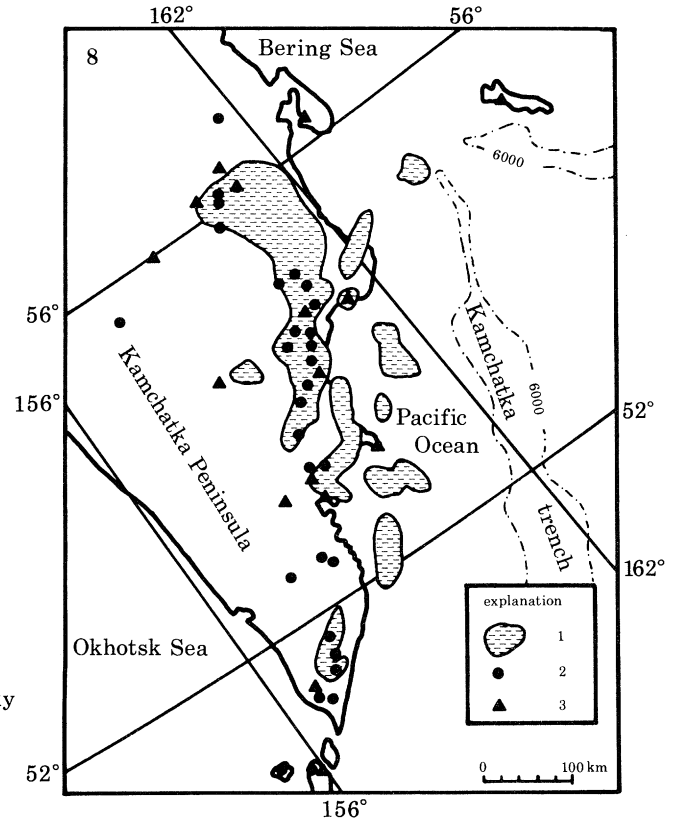

FIGURE 7. Ratio of average amplitude A and period T of SH-waves at station Topolev (Top) normalized to the ratio at reference station Petropavlovsk (Ptr), plotted as a function of azimuth of earthquake epicentre from 'Top'. H denotes depth of earthquake focus. Subscript s denotes use of SH-waves. Locations of volcanoes are also shown. (Adapted from Farberov & Gorelchik 1971.)

FIGURE 8. Approximate zones which screen P- and S-waves at depths of 30–100 km in the upper mantle beneath Kamchatka. 1: Zones of P- and S-wave alternation; 2: volcanoes; 3: seismic stations. (Adapted from Fedotov 1973.) Copyright The University of Western Australia Press.

Farberov *et al.* (1979) located several magma chambers under the Kamchatka volcanoes with the diffraction technique. By plotting the seismic shadows observed at many stations from earthquakes in different azimuths, they delineated an anomalous zone under the Avacha–Koryasky volcanic group in the depth interval 30–90 km. The horizontal dimensions of the bodies were in the range 8 km by 15 km to 15 km by 40 km.

Firstov & Shirakov (1971) investigated the screening effect of both P- and S-waves from intermediate focus earthquakes in the Klyuchevskaya volcanic region, and identified anomalous zones, inferred as magma chambers at depths of 35–80 km.

Fedotov (1973) used a somewhat different approach, based on P- and S-wave absorption, to determine the probable areas of magma concentration under the Kuril–Kamchatka arc.

The method is based on computing the deviation in P- and S-wave energy, with reference to a regional average, on seismograms from the region. Assuming that the energy decreases were caused by 'shadows' of magma bodies, using diffraction theory, they located the positions of the bodies. The zones of P- and S-wave screening in the Kamchatka region are shown in figure 8. The map, the first of its kind in the world, shows the locations of the anomalous regions on the surface, the actual depths of the anomalies being in the range of 30–100 km.

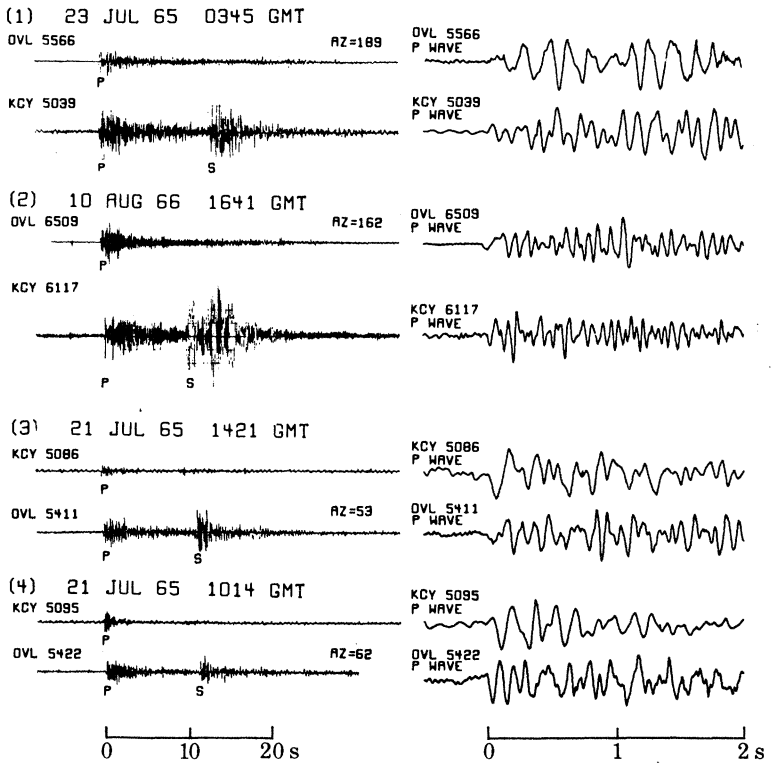

FIGURE 9. Seismograms showing S-wave attenuation at stations OVL and KCY in the Katmai region, Alaska. The first two seconds of P-waves of corresponding seismograms are shown on the right side of the figure in an expanded time scale to highlight the apparent increase in period of P-waves (Matumoto 1971).

The seismic wave attenuation method was used by Kubota & Berg (1967) and Matumoto (1971) to identify magma chambers in the Katmai volcanic region, Alaska. Kubota & Berg used a three-station seismic network together with a reference station at Kodiak Island, and found that in many cases SV-waves were screened, while SH-waves were transmitted. These phenomena were attributed to the presence of magma chambers in the shape of oblate spheroids.

Perhaps the best discussion on the use of the S-wave attenuation technique to locate magma pockets is that given by Matumoto (1971). He operated two high-gain, high-frequency, tripartite arrays with a spread of approximately 750 m between geophones, 15 km to the west and 5 km to the south of Mt Katmai. Spectacular differences were seen in the seismograms at the two stations as shown in figure 9. Note that in each of the four pairs of seismograms, clear S-waves are seen at one of the two stations while only P-waves are recorded at the other station. Also, the P-waves at the stations showing no shear waves are characterized by an increase in apparent period, as shown in the expanded time scale on the right. When the earthquake epicentres were plotted relative to station locations separating the normal and

anomalous paths, it became clear that the anomalous paths were associated with three distinct areas in the vicinity of the active volcanoes in the region. Hence, the shear-wave disappearance was attributed to the presence of magma pockets under the volcanoes. The use of seismic arrays enabled the determination of apparent velocities of the P-waves, which are directly related to the depth of the anomalous zones. Using the surface projections of locations of the anomalous zones by ray plotting, and determining their depths by using apparent

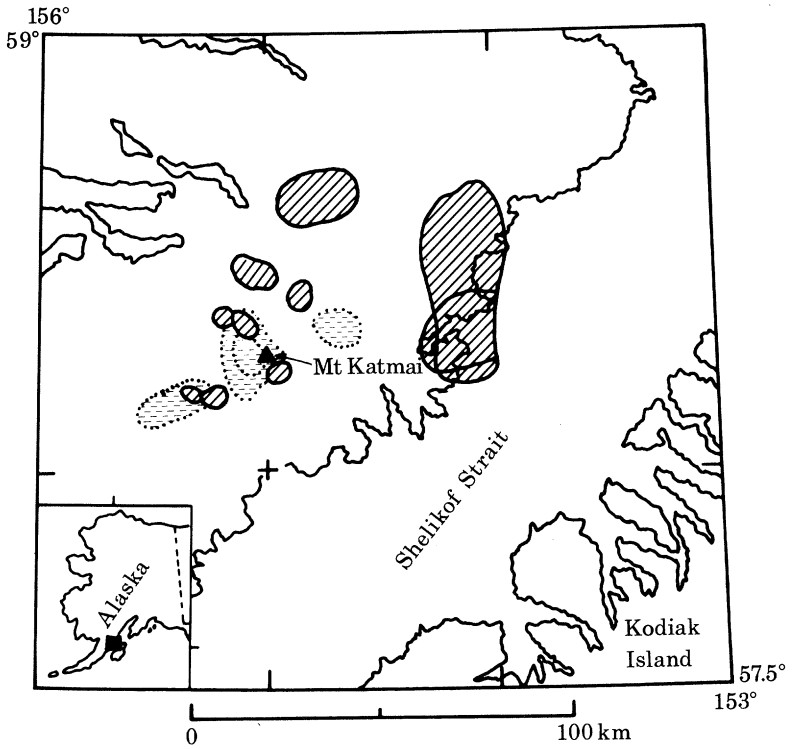

FIGURE 10. Locations of magma chambers in the Mt Katmai region, Alaska. The depth varies from very shallow to 40 km. Dashed areas with solid line boundaries are magma chambers outlined by Kubota & Berg. Stippled areas bounded by dots represent magma chambers detected by Matumoto. (Adapted from Kubota & Berg 1967 and Matumoto 1971.)

velocities, Matumoto located four magma chambers near Mt Katmai, Alaska (figure 10). Three chambers were located directly beneath volcanic vents and one chamber coincided with the zone of an earthquake swarm which occurred in 1965. The first three were located at depths shallower than 10 km, but the fourth was at a depth of 20–30 km. Magma chambers in the Katmai region, located by Kubota & Berg (1967) are also shown in figure 10 for comparison. Matumoto did not have to assume the shapes of the magma pockets to be oblate spheroids to explain the difference in the amplitudes of SV- and SH-waves. He showed that the differences in amplitudes of SV- and SH-waves observed by Kubota & Berg (1967) could be explained by the shift in the shadow boundary of SV- and SH-waves arising from diffraction. Matumoto used the observed attenuation to calculate viscosity in the melt. Assuming a model in which melt occurs in thin films along grain boundaries, he calculated normalized spectra of S-waves for various values of the coefficient of viscosity. Assumptions were made on the dimensions of the magma body, percentage of melt concentration, elastic coefficients, and seismic velocities in the melt and solid rock, to compute the spectra. Comparison of the observed and theoretical spectra showed that the best fit occurred for a viscosity value of about 10^8 cgs units.

PHILOSOPHICAL TRANSACTIONS OF THE ROYAL SOCIETY A MATHEMATICAL, PHYSICAL & ENGINEERING SCIENCES

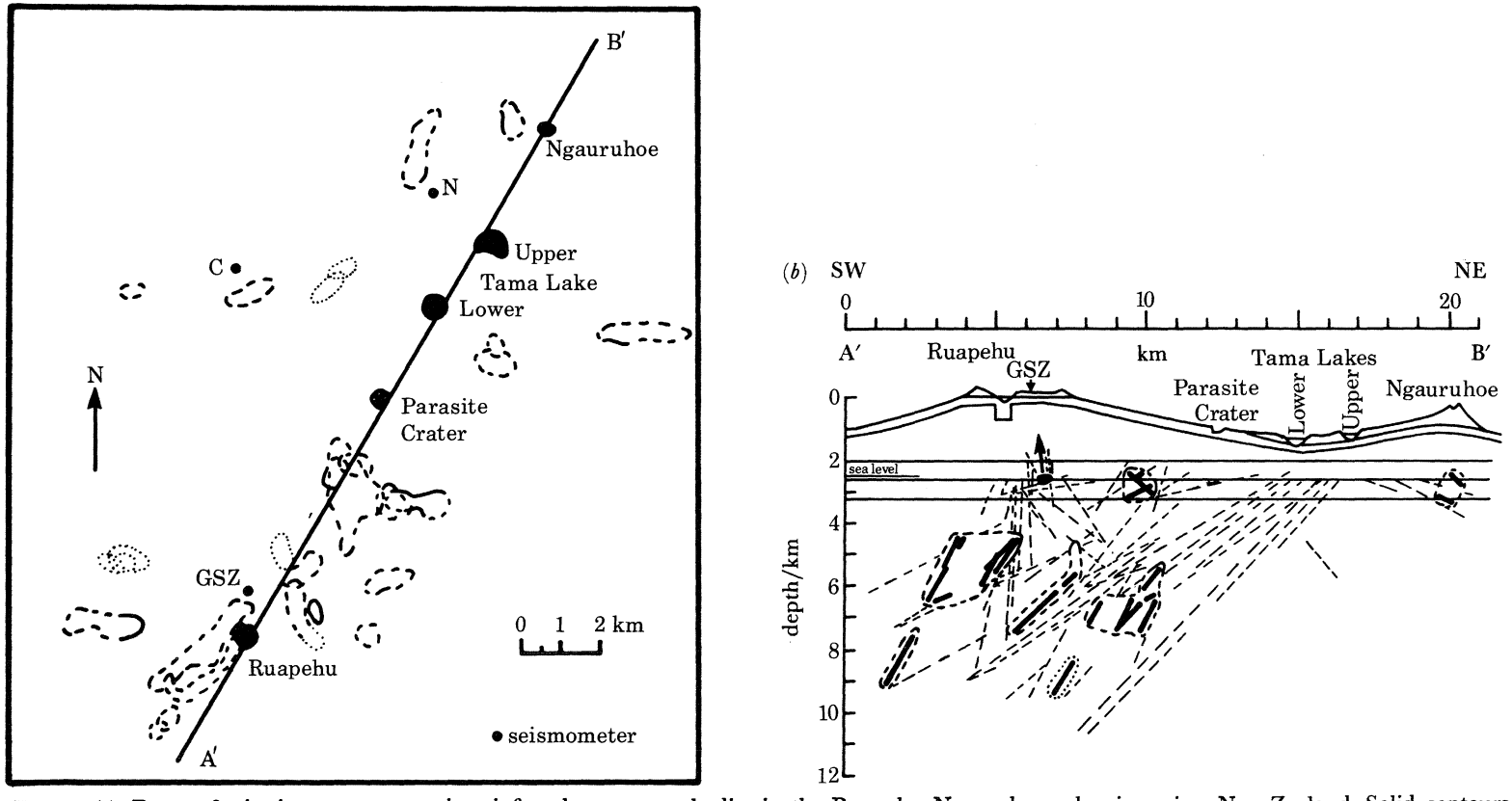

FIGURE 11. Zones of seismic wave attenuation, inferred as magma bodies in the Ruapehu–Ngauruhoe volcanic region, New Zealand. Solid contours denote well established boundaries, short dashed contours moderately well established boundaries, and dotted contours poorly defined boundaries. (*a*) Map view: the dark zones indicate geographic features shown along side; GSZ, C, and N are seismometer locations. (*b*) Cross section along A′–B′ showing some of the magma bodies: dashed lines indicate attenuating ray paths and heavy lines severely attenuating segments of ray paths. The heavy arrow indicates abnormal attenuation at shallower levels in the direction shown. (Adapted from Latter 1981.)

Einarsson (1978) used S-wave disappearance in seismograms from earthquakes associated with the inflation of the Krafla volcano in Iceland to locate two zones of high attenuation with 1–2 km horizontal diameter within the Krafla caldera. Since the earthquake distribution showed a decrease in number at a depth of 3 km, the top of the attenuating body was estimated to be somewhere around that depth. The lower boundary was inferred to be probably shallower than 7 km because three deeper earthquakes showed no shear-wave attenuation. Einarsson suggests that the magma may be occurring in the form of interconnected chambers, sills or dikes.

Latter (1981) used the frequency reduction of S-waves from local earthquakes to map magma bodies in the Ruapehu and Ngauruhoe volcanoes in the Tongariro National Park, central North Island, New Zealand. He computed the ratio of the dominant frequency of P-waves to S-waves and if the values were above an empirically determined threshold value, they were considered anomalous. Using more empirical procedures, Latter identified over 25 anomalous bodies in the region (figure 11*a*). A typical southwest–northeast cross section, indicating some of the magma bodies is shown in figure 11*b*.

Ryall & Ryall (1981) have documented the disappearance of shear waves and absorption of high frequency P-waves in Long Valley, California, where abnormal seismic activity since 1980 is believed to be associated with a resurgence of magmatic activity. Teleseismic delay studies and other geophysical data indicate the presence of a large magma chamber under the Long Valley caldera (see §5.5.3). They postulate the presence of partially melted rock at a depth greater than 7–8 km, the depth of earthquakes used in the study.

5.3. *Reflected phases from earthquakes*

The first discovery of a magma body near Socorro, New Mexico, in the Rio Grande Rift, U.S.A., was made by the use of reflected phases from local earthquakes. (For a discussion of a Vibroseis reflection study of this magma body see §4.5.) Sanford & Long (1965) reported that in the seismograms of local earthquakes near Socorro, about 25% of the events had, in addition to the usual P- and S-phases, two sharp arrivals which followed the direct S by 2.5 and 5.0 s (figure 12*a*). They interpreted these arrivals as reflections of the S-phase from a crustal discontinuity at a depth of about 18 km. In subsequent detailed studies, Sanford *et al.* (1973) and Rinehart *et al.* (1979) estimate the depth of the reflecting surface to be 19 km. They demonstrated that the observed data fit reflections from a magma discontinuity rather than from the Conrad discontinuity. By plotting the reflection points they estimated the aerial extent of the body to be approximately 1200 km^2 (figure 12*b*). Sanford & Einarsson (1982) have provided additional evidence to show that the reflector was indeed a magma body. These are: evidence of more or less continuous uplift at a rate of about 5 mm a^{-1} as determined from several level lines in the region of the rift near Socorro; presence of frequent earthquake swarms; and high heat flow. The authors prefer the interpretation that the magma chamber is a large sill caused by intrusion of basalt rather than being caused by *in situ* melting of granite.

5.4. *Three-dimensional modelling by using local earthquakes*

Ward *et al.* (1981) have applied this method to study the magma body in the Socorro region in New Mexico (§§4.5 and 5.3). By using P-wave arrival times from a portable seismic array, and by assuming an initial Earth model, a set of linearized equations were generated in terms of the differences between observed and theoretical arrival times at the stations and velocity

perturbations in a volume divided into three-dimensional blocks. Solving for the velocity perturbations resulted in a velocity model that showed that one block in the lower layer, 4–10 km deep, had an abnormally low velocity of 5.17 km s^{-1} compared with the average regional velocity of 5.85 km s^{-1}. Ward *et al.* have interpreted this low velocity to be the result of a magmatic intrusion associated with the large magma body at 19 km depth found in Socorro by Sanford *et al.* (1973).

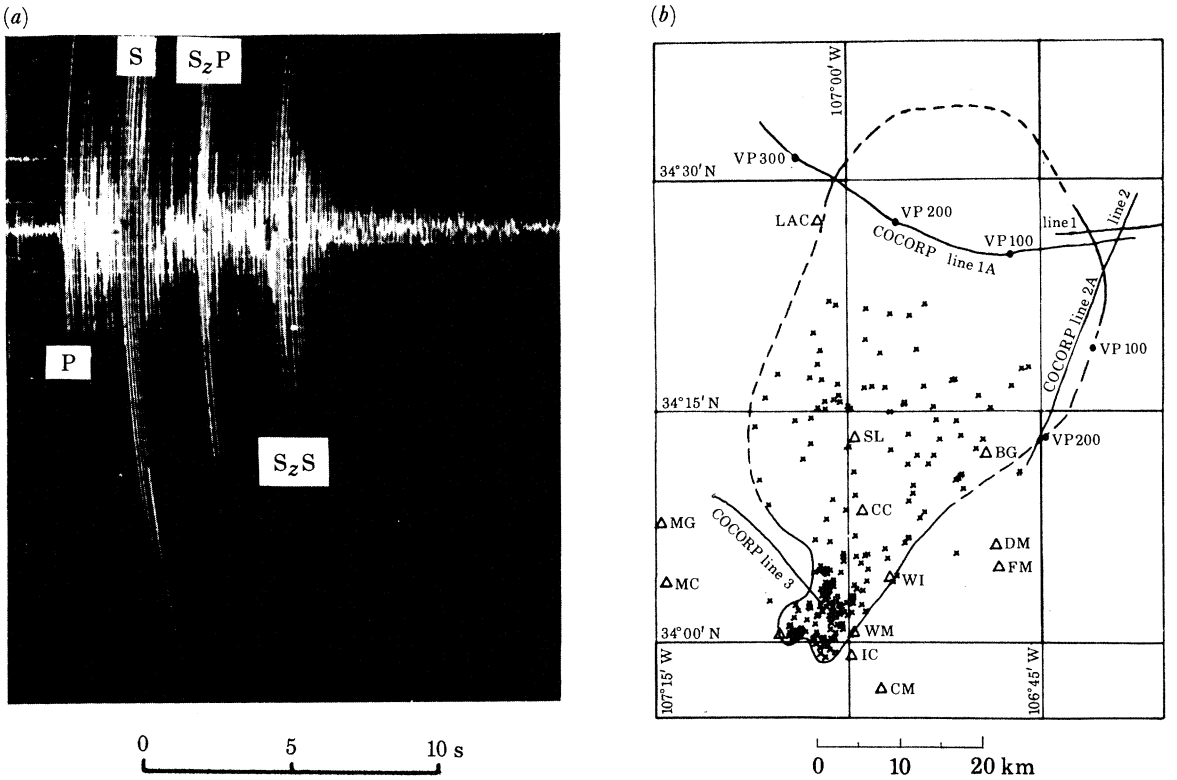

FIGURE 12. (*a*) A micro-earthquake seismogram in the Socorro region, New Mexico. P- and S-phases and sharp reflected phases S_zP and S_zS are seen. (*b*) A map of well located reflection points. Boundaries of the inferred sill-like magma body are shown by solid lines where well constrained and dashed lines were poorly constrained. Triangles show seismic stations. Also shown are the Vibroseis reflection profiles (Rinehart *et al.* 1979). Copyright American Geophysical Union.

In a recent study, Akiko Horie (personal communication) constructed a three-dimensional model of the Tohoku district, Japan by inversion of arrival times from local earthquakes. She finds a low-velocity region at a depth 65 km beneath the volcanic front and interprets it as a magma zone.

5.5. *Teleseismic* P-*wave residual* (P-*delay*) *technique*

This technique was first used to explore for magma in Yellowstone National Park, Wyoming (Iyer 1975) and in Long Valley, California (Steeples & Iyer 1976). The P-delay technique has subsequently been used in the U.S.A. to detect magma chambers in several areas of Quaternary volcanism, to study the deep structure of the Cascade volcanoes, and to evolve volcano-tectonic models of the Oregon and Washington Cascades and Hawaii. A significant contribution to the success of the technique was the development of a linear inversion technique by Aki *et al.* (1976, 1977) to obtain three-dimensional velocity models from P-wave residuals.

Arrival times of seismic P-waves from distant earthquakes (teleseisms) occurring at distances greater than 2000 km provide the basic data for these studies. The seismic waves reach the recording stations at angles varying from almost vertical for the very distant events to about 30° to the vertical for events at a distance of about 2000 km. Travel-time residuals are computed with one of several available earth models. In order to correct for source-location errors, errors in travel-times caused by deviations in structure of the real earth from the 'standard earth' used in the tables, and lateral heterogeneities along the ray path other than those under the seismic network, a reference residual is subtracted from the computed residuals to obtain relative residuals. The spatial pattern of relative residuals contains the required information on the shape and magnitude of the velocity anomaly under the seismic network.

For quantitative modelling of the P-residuals the three-dimensional inversion technique developed by Aki *et al.* (1976, 1977) is used. In this technique, the earth under the seismic array is divided into rectangular blocks, the block dimensions being determined primarily by the average station spacing in the seismic network. The starting model is a stack of homogeneous plane-parallel layers overlying a standard earth. The velocities in the blocks are now perturbed which results in travel time changes within each block, which when summed along the ray path gives a result equal to the observed residuals. Thus, for events from many azimuths recorded at the stations in the network, a series of linear equations are generated relating the observed residuals and the perturbation of velocity in each block. The equations are solved by using a damped least-squares inversion technique. The final result is in percentages of velocity perturbations for each block.

The volcanic areas where the P-delay experiments of the U.S. Geological Survey were carried out are shown in figure 13. A brief summary of the important results is given below.

5.5.1. *Yellowstone National Park, Wyoming*

Yellowstone National Park, Wyoming, is at the northeast end of the Snake River Plain–Yellowstone volcanic sub-province. Yellowstone caldera is a large rhyolitic centre and is considered by some to be the current location of a hot spot. Using 100 teleseisms recorded by a network of 55 permanent and portable seismic stations, Iyer *et al.* (1981) found strong, azimuthally dependent, relative delays (positive residuals) as large as 2 s, in a region of approximately 150 km radius centred on the Yellowstone caldera. Using ray-plotting techniques and the three-dimensional inversion technique, they showed that the delays were caused by a large, deep low-velocity body under the Yellowstone caldera. They estimated the body to extend from the upper crust to a depth of about 250 km. The P-wave velocity inside the body was lower than in the surrounding normal region by 8–15% in the upper crust, 5% in the lower crust, and 2–4% in the upper mantle (figures 14, 15*a*). Iyer & Stewart (1977) and Iyer *et al.* (1981) interpreted the low velocity body to be a large magma chamber responsible for the volcanism in Yellowstone.

The Bouguer gravity map of the Yellowstone National Park region is dominated by a large gravity low with a maximum closure of 50 mGal and an elliptical shape almost coinciding with the boundary of the Yellowstone caldera (1 Gal = 1 cm s^{-2}). Evoy (1978) and Savino *et al.* (1979) did a simultaneous inversion of gravity and teleseismic residual data of Iyer *et al.* and found density contrasts of -0.1 to $+0.1$ g cm^{-3} in the top 10 km of the crust, -0.05 to -0.15 for 10–60 km depth, and -0.05 to -0.10 for 60–100 km depth (figure 15*b*). In general, Evoy's density contrasts for the lower crust and upper mantle are somewhat less than the percentage

PHILOSOPHICAL TRANSACTIONS OF THE ROYAL SOCIETY A MATHEMATICAL, PHYSICAL & ENGINEERING SCIENCES

PHILOSOPHICAL TRANSACTIONS OF THE ROYAL SOCIETY A MATHEMATICAL, PHYSICAL & ENGINEERING SCIENCES

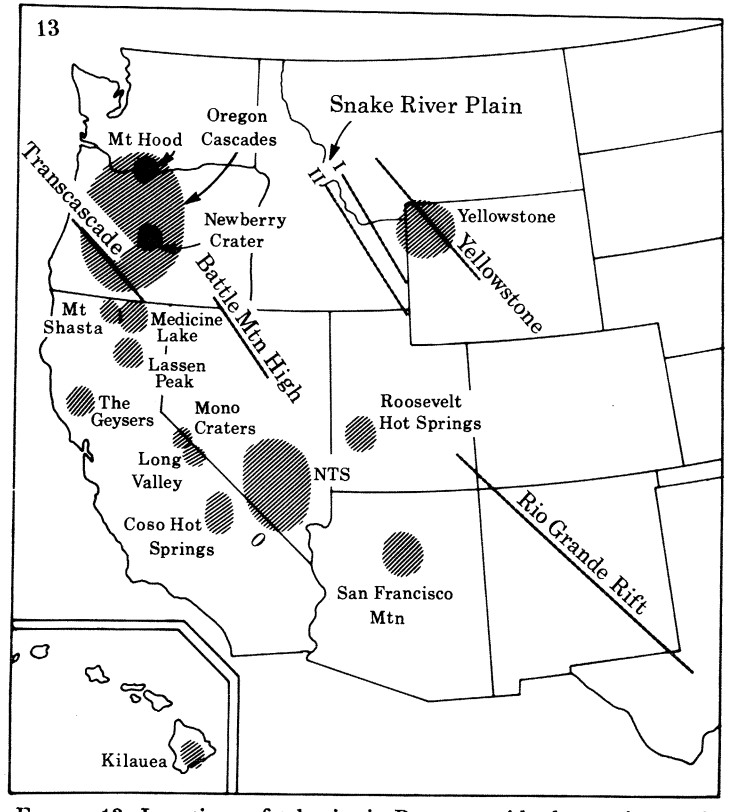

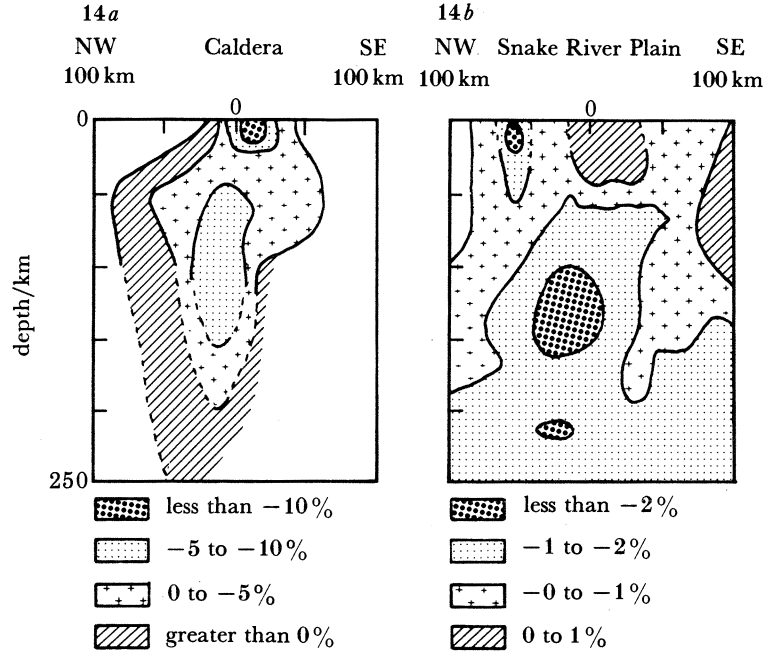

FIGURE 13. Locations of teleseismic P-wave residual experiments in volcanic areas done by the U.S. Geological Survey. Shaded areas represent approximate regions covered by seismic networks; lines are profiles of seismic stations; names of volcanic features studied are indicated.

FIGURE 14. Northwest–southeast P-wave velocity anomaly cross sections of Yellowstone National Park and Eastern Snake River Plain. Contours represent percentage change relative to surrounding region. (*a*) Yellowstone, adapted from Iyer *et al.* (1981); contour interval 5%. (*b*) Eastern Snake River Plain, adapted from Evans (1982); contour interval 1%.

decrease in P-wave velocity found by Iyer *et al.* The joint inversion was able to delineate a zone of abnormally low density in the top 10 km of the crust in the vicinity of the Mallard Lake and Sour Creek resurgent domes (not shown). Note that the fan-shooting data (see §4.2) also showed a strong velocity contrast under the Sour Creek resurgent dome.

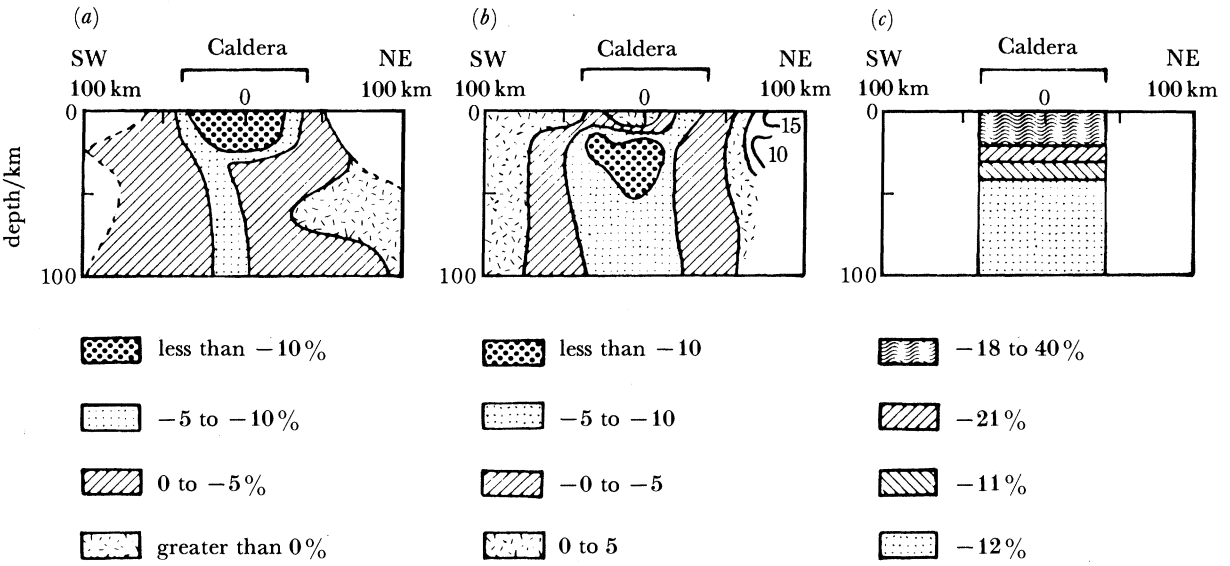

FIGURE 15. Southwest–northeast cross sections of seismic wave velocity and density anomaly models for Yellowstone region. (*a*) P-wave velocity, Iyer *et al.* (1981); contour interval 5%. (*b*) Density in units of 0.01 g cm^{-3}, Evoy (1978). (*c*) S-wave velocity, Daniel & Boore (1982).

If significant volumes of partial melt are present beneath the Yellowstone caldera, we should expect to see exceptionally low shear wave velocities. Daniel & Boore (1982) did indeed find abnormally low shear wave velocities in Yellowstone. Using a tripartite seismograph network of intermediate period instruments in the caldera and a reference station outside, they found S-delays of about 5 s, twice as much as the P-delays found by Iyer *et al.* The S-delays were interpreted as being due to an average velocity decrease of about 9% from the surface to 200 km under the Yellowstone caldera.

In the final model of Daniel & Boore (figure 15*c*), the velocity contrast is −18 to −40% in the upper crust, −11 to −21% in the lower crust, and −12% in the upper mantle. This model was confirmed by S-wave models obtained by using Raleigh wave phase velocities measured by the tripartite array.

The above data and additional geophysical data reviewed by Iyer (1983) show clearly the presence of a large volume of magma in the Yellowstone lithosphere with localized manifestations in the upper crust.

5.5.2. *Eastern Snake River Plain, Idaho*

In the Eastern Snake River Plain–Yellowstone region the propagation of rhyolitic centres from southwest to northeast occurs at a rate of approximately 3.5 cm a^{-1} (Armstrong *et al.* 1975). Evans (1982) operated two teleseismic profiles in Idaho across the Eastern Snake River Plain at locations where rhyolitic volcanism began approximately 3 to 6 million years ago. In both profiles Evans found 1–2 s relative delays, their azimuthal pattern indicating that the delay-causing anomaly was in the upper mantle. Using a two-dimensional version of the linear inversion scheme, Evans modelled a large, low-velocity body, approximately 100 km wide

under the Eastern Snake River Plain. The velocity inside the body was lower than in the surrounding mantle by 2–4% (figure 14*b*). Interesting aspects of the model were the absence of any large-scale velocity anomalies in the crust and the similarity of the Eastern Snake River Plain and Yellowstone models in the deep lithosphere and the asthenosphere. Evans interpreted these phenomena as the ageing process of the Eastern Snake River Plain–Yellowstone system.

5.5.3. *Long Valley, California*

Long Valley, located east of the Sierra Nevada in California, is a collapse caldera which formed 700000 years ago with a history of recent volcanic activity. Steeples & Iyer (1976), using teleseismic data and simple ray-plotting techniques, inferred the presence of a low velocity body of 10–15 km diameter with a velocity contrast of 10–15% under the caldera (figure 16*a*). Since 1980, unusually high seismic activity, consisting of several earthquakes with magnitudes higher than 5 and earthquake swarms, have occurred in the southwestern part of the Long Valley caldera. Also, Savage & Clark (1982) have measured an uplift of about 25 cm during the period 1975–80 and interpreted it to be consistent with the inflation of a magma reservoir. These findings are important in the present context of magma chamber detection because they provide a direct verification that the low velocity anomaly found by Steeples & Iyer is indeed a magma chamber.

5.5.4. *The Geysers–Clear Lake volcanic field, California*

The Geysers–Clear Lake volcanic field, ranging in age from 10000 years to 2 million years, has within it the Geysers geothermal field which is currently generating about 1000 MW of electricity. For a long time it has been suspected that a large magma chamber was responsible for the volcanic and thermal phenomena observed here. Isherwood (1976) modelled the strong gravity low in the region as a low-density body in the crust and inferred it to be a magma chamber (see §6). Iyer *et al.* (1981) found relative delays in the range of 0.5–1.5 s in the Geysers–Clear Lake volcanic field and modelled them as a magma chamber under the volcanic field and a low-velocity body under the steam zone. They found the velocity decrease to be as high as 25%, which implies the presence of an intense zone of partial melting. Oppenheimer & Herkenhoff (1981) modelled the teleseismic data using 3D inversion and obtained a quantitatively rigorous model of the low-velocity anomaly. An east–west cross section of the anomaly is shown in figure 16*b*. The low-velocity body encompasses the steam field and the volcanic field and extends from the crust to the upper mantle to a depth of about 60 km, with an average velocity decrease of about 12% in the crust and 2% in the upper mantle. Oppenheimer & Herkenhoff carried the velocity inversion a step further and predicted the gravity low using the velocity model by solving for a relation between gravity and density perturbations. They found that the teleseismic delays and gravity anomaly (at least the long wavelength component of it) were caused by the same body and that a density decrease of about 15% was needed to explain the anomaly.

5.5.5. *Coso Geothermal Area, California*

Reasenberg *et al.* (1980) measured the teleseismic residuals in this region of recent volcanism. An interesting aspect of this study was that a dense, 16-station seismic network, operated in the region for seismicity studies, was not able to provide clearly identifiable residual patterns which could be related to the presence of a low-velocity anomaly. However, with a more dense

PHILOSOPHICAL TRANSACTIONS OF THE ROYAL SOCIETY A MATHEMATICAL, PHYSICAL & ENGINEERING SCIENCES

portable seismic network they found an azimuthal pattern of relative residuals which could only be explained as a delay shadow caused by a low-velocity body at depth. Three-dimensional inversion showed the body to be in the depth range of 5–20 km, with a maximum velocity contrast of about 8%. Further, it showed the body to be approximately 5 km in lateral size and located under the active geothermal area (figure 16*c*).

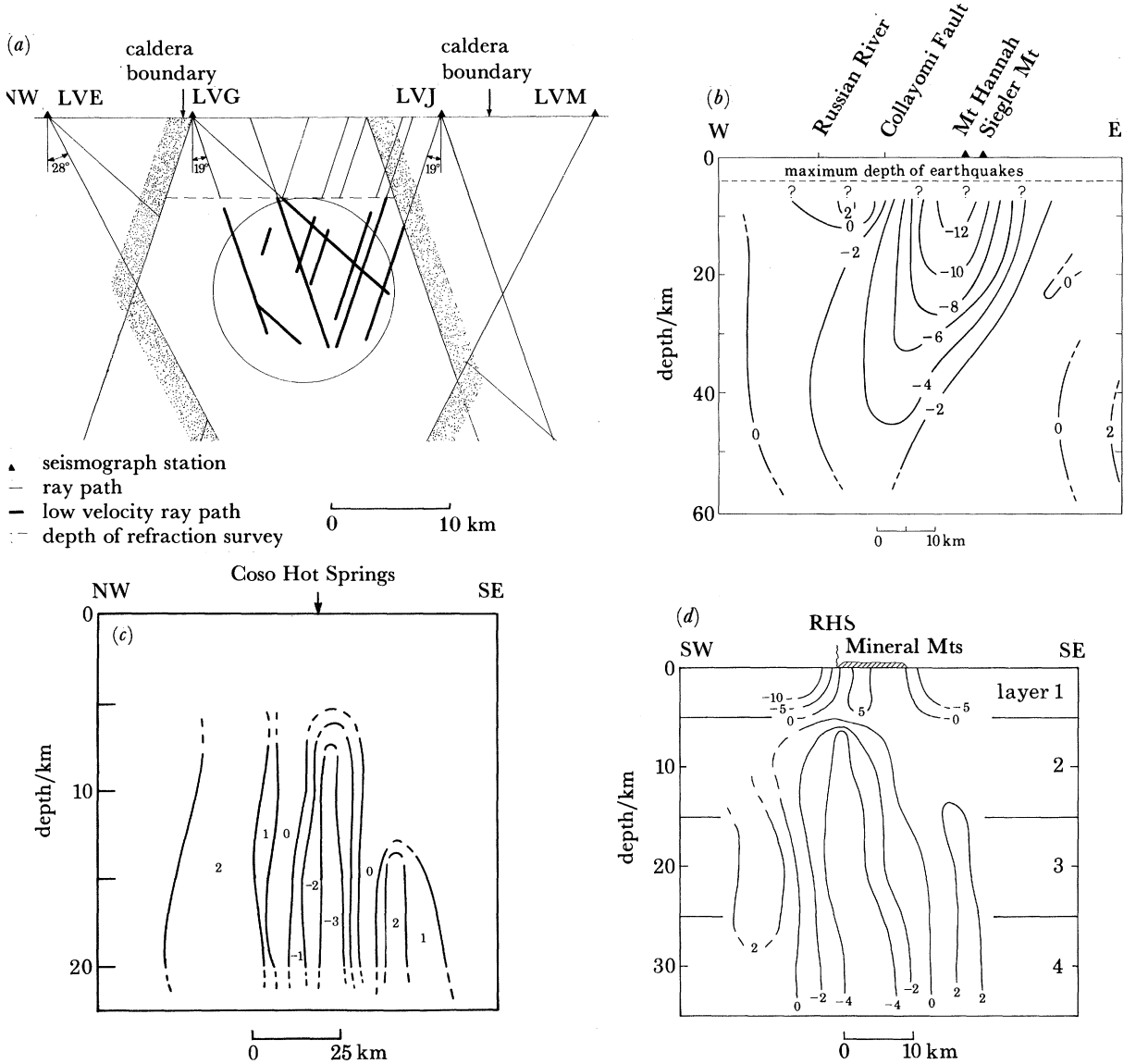

FIGURE 16*a*, *b*, *c* and *d*. For legend see facing page.

5.5.6. *Roosevelt Hot Springs geothermal area, Utah*

The teleseismic delay study in this region by Robinson & Iyer (1981) demonstrates the importance of a carefully designed geometry for the seismic network and the power of the three-dimensional inversion method in separating velocity anomalies in the crust due to geologic structure and in the lower crust and upper mantle due to a magma body. The Roosevelt Hot Spring area is located on the flanks of a granitic pluton with alluvial valleys on either side. A closely-spaced, two-dimensional array of 15 seismic stations was operated in the area to

PHILOSOPHICAL TRANSACTIONS OF THE ROYAL SOCIETY A MATHEMATICAL, PHYSICAL & ENGINEERING SCIENCES

study the source of the recent rhyolitic intrusions and the geothermal phenomena (figure 17*a*). The results of the three-dimensional inversion shown in figure 17*b* demonstrates how in the top 5 km of the crust the obvious features are the surficial low velocities characteristic of the alluvial valleys on either side of the pluton. However, note that in the second to fourth layer

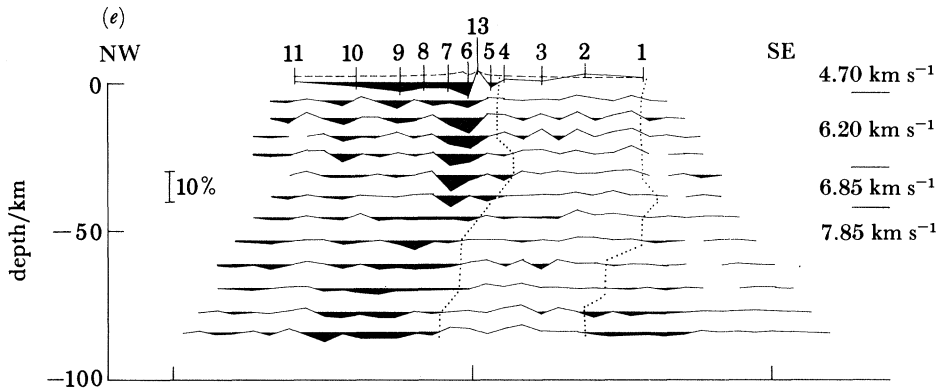

FIGURE 16. Low-velocity bodies in volcanic areas determined with teleseismic residuals and inferred as magma chambers. (*a*) Long Valley, California. The circle is a cross section of a spherical low-velocity body in which the P-wave velocity is lower than in the surrounding rock by 15%. Heavy lines are segments of anomalous ray paths. Velocity outside the stippled zone defined by 'normal' ray paths corresponds to regional crustal velocity (Steeples & Iyer 1976). (*b*) East–west cross section of velocity anomaly model of the Geysers-Clear Lake volcanic region, California. Contours are perturbations in P-wave velocities, interval 2% (Oppenheimer & Herkenhoff 1981). (*c*) Coso geothermal area, California. Contour interval 1% (Reasenberg *et al.* 1980). (*d*) Roosevelt Hot Springs, Utah. Contour interval is 2% (Robinson & Iyer 1981). (*e*) San Francisco volcanic field, Arizona. For each layer in the model, horizontal variations in velocity perturbations are indicated by vertical offsets. The amplitude scale for 10% perturbations is shown at left. Velocity perturbations below the mean layer velocity are shaded. Regional crustal velocity model is shown at right (Stauber 1982). (*a*), (*b*), (*c*) and (*e*) are copyrighted by the American Geophysical Union.

extending from 5–35 km depth the low velocities in the top layer have been completely stripped off and a low velocity body centred near the geothermal area is delineated. The body has a maximum velocity contrast of about 7% from the surrounding rock and can be traced from about 5 km depth to 35 km (figure 16*d*). In this case, as in the previous cases discussed, the teleseismic studies clearly show that the low-velocity (magma) bodies extend from the upper crust into the upper mantle. This phenomenon may be providing an important clue that the identified magma chambers are not isolated pockets in the crust but are connected to feeder channels in the mantle.

5.5.7. *San Francisco volcanic field, Arizona*

By stretching the usefulness of the inversion technique to its limits by careful choice of the block model and paying attention to the resolutions, Stauber (1982) identified a low velocity body under San Francisco Mountain, a stratovolcano in Arizona. He used a 250 km long northwesterly profile across the volcanic field to look for the localized anomalies associated with the volcano and broad regional anomalies in the mantle. However, the only anomaly he found was a 6 km wide, low-velocity body extending from 9–34 km under the stratovolcano. The velocity decrease in the body was about 6% with respect to the surrounding rock (figure 16*e*). Using available laboratory and petrological data, Stauber made a detailed analysis of the possible causes of the anomaly and suggested four possible interpretations: (1) cooling

PHILOSOPHICAL TRANSACTIONS OF THE ROYAL SOCIETY A MATHEMATICAL, PHYSICAL & ENGINEERING SCIENCES

PHILOSOPHICAL TRANSACTIONS OF THE ROYAL SOCIETY A MATHEMATICAL, PHYSICAL & ENGINEERING SCIENCES

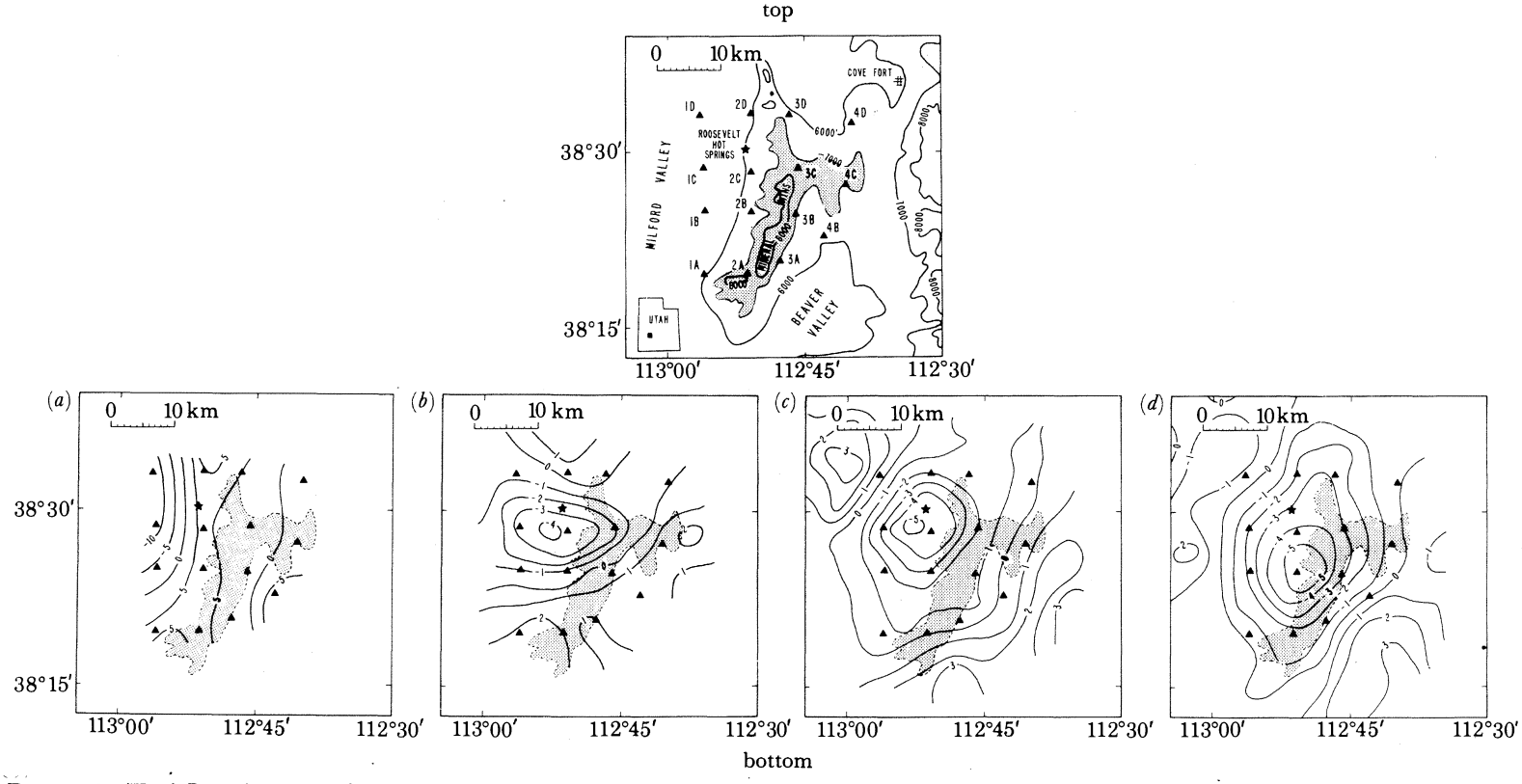

FIGURE 17. (Top) Location map of Roosevelt Hot Springs geothermal area, Utah. Triangles are seismic stations used in the teleseismic survey. Elevation contour interval 1000 ft (305 m). (Bottom) Contours of P-wave velocity perturbations. For the first layer,the contour interval is 5%; for the others, it is 1%. Star indicates the location of Roosevelt Hot Springs. Dashed line shows outline of Mineral Mountain. (*a*) Layer 1: 0–5 km; (*b*) layer 2: 5–15 km; (*c*) layer 3: 15–25 km; (*d*) layer 4: 25–35 km (Robinson & Iyer 1981).

granitic pluton in a basaltic crust; (2) velocity change due to a quartz transition in high temperature rock; (3) a high density of water-filled cracks; and (4) presence of partial melt. Whatever the cause of the anomaly the results show a long, conduit-like, low velocity body directly beneath the stratovolcano.

5.5.8. *Mount Etna, Sicily*

Sharp *et al.* (1980) have located a magma chamber under Mt Etna, Sicily, using travel-time residuals. The fourteen events used in this study were not teleseismic, but were regional events in the distance range of 70–1000 km. The observed residuals were modelled to fit a triaxial, ellipsoidal magma chamber under the volcano. Eight parameters, the three ellipsoid axes, depth to the centre of the ellipsoid, orientation of the ellipsoid, and velocity decrease within the ellipsoid were systematically varied and, from over 20000 trial models, the best-fitting model was chosen. The best constrained values were the major (horizontal) axis of the ellipsoid, found to be 22 km, and depth, found to be 20 km. The velocity decrease could be 15–30% and the thickness and shorter horizontal axis from 2–8 km.

5.5.9. *Cascade Volcanoes, California and Oregon*

In contrast to the low-velocity anomalies, inferred to be magma chambers, found in several regions of Quaternary volcanism in the U.S.A., teleseismic experiments in the Cascade volcanoes of the western United States have consistently failed to show any magma chambers. At Mt Hood (Weaver *et al.* 1981), Newberry Volcano (Iyer *et al.* 1982), Mt Lassen (Mary Monfort, personal communication), and Mt Shasta (Douglas Stauber, personal communication), detailed and careful teleseismic residual experiments have not shown the presence of low velocity anomalies beneath the volcanoes. One possible explanation is that the magma chambers may be of small size, only a few cubic kilometres. The resolution of the teleseismic technique is about 5 km horizontally and vertically.

Even though it is known that the origin of Cascade Volcanoes is associated with the subduction of the Juan De Fuca plate very little geophysical clues exist as to processes of magma generation and storage in the region. Inversion of teleseismic residual data from a 32-station regional network in the Oregon Cascades has given some clues on the parental magma source in the region. A three-dimensional velocity model with data from this network suggests an inclined zone of high velocity material, suggestive of a subduction zone, with lower-than normal velocity above it (Iyer *et al.* 1982). The model is interpreted as an underthrusting lithosphere with shear-heated material rising above it and indicates the presence of a parental source of magma in the lower crust and upper mantle beneath the Cascades. The lack of detectable magma chambers under individual volcanoes shows that the magma rises to the surface through narrow conduits and is stored only in small pockets in the upper crust.

5.5.10. *Kilauea Volcano, Hawaii*

Ellsworth & Koyanagi (1977) modelled the P-wave velocity under Kilauea Volcano, Hawaii, using teleseismic data from a regional network. The results showed no evidence for the presence of low velocity material in either the crust or mantle to depths of about 40 km. The authors speculate that the magma source in Hawaii is therefore deep and magma is fed by an extensive but narrow conduit system to the summit of the volcanoes and the fissures (see also §5.1).

PHILOSOPHICAL TRANSACTIONS OF THE ROYAL SOCIETY A MATHEMATICAL, PHYSICAL & ENGINEERING SCIENCES

5.6. *Teleseismic* P-*wave attenuation*

The teleseismic data collected for P-wave residual studies in the Geysers–Clear Lake, Coso, and Roosevelt Hot Springs geothermal areas (see §§5.5.4, 5.5.5, and 5.5.6) were used to study attenuation anomalies in these areas by Ward & Young (1980) and Young & Ward (1980, 1981) who used a spectral analysis technique. They showed that the ratio of spectra of P-waves at a station located over the anomaly under investigation and at a reference station is linearly related to a quantity called the differential attenuation factor which in turn is related to Q^{-1} which is a dimensionless parameter indicating the fraction of the energy dissipated per cycle by a seismic wave. The parameter Q^{-1} thus measures the anelasticity of a solid and is sensitive to mechanisms that attenuate seismic waves, such as partial melting, grain boundary relaxation, internal friction, etc. It is convenient to describe the attenuating property of rocks in terms of Q rather than Q^{-1}. For typical crustal rocks Q is on the order of 1000 and for partial melts it could be as low as 10.

In a study of attenuation in the Geysers area, Ward & Young (1980) used a linear inversion procedure to obtain a two-dimensional Q-model from spectral ratios and found a high-attenuating (low Q) zone at mid-crustal depths, which approximately coincided with the region of low-density and low-velocity found by gravity and P-delay studies (see §5.5.4). A three-dimensional Q-model for the Coso geothermal area (Young & Ward 1980), showed no evidence for a low-Q zone corresponding to the magma chamber delineated by Reasenberg *et al.* (1980) using P-wave delays. In the Roosevelt Hot Springs area, there is evidence for a shallow low-Q zone in the upper crust beneath the geothermal area (C. Young & R. W. Ward, personal communication).

The technique of modelling Q using teleseismic waves is perhaps as powerful as the P-delay technique in detecting magma chambers and when the two techniques are used together they could provide good constraints for interpretation of the degree of partial melting. However, the full potential of the technique has not been used so far, probably because the data sets are not adequate.

6. Gravity

The application of gravity techniques to study magma chambers is illustrated by Isherwood's (1976) interpretation of the large gravity anomaly in the Geysers–Clear Lake area, California (see §5.5.4). A detailed residual gravity map of the region shows a gravity low centred on Mount Hannah located at the south-west edge of the Quaternary volcanic field, with a secondary low centred on the steam production zone (figure 18*a*). Isherwood estimated that a sphere with its centre at a depth of 13.5 km would best fit the low-pass filtered gravity data. The diameter of the sphere could be varied, depending upon the specified density decrease inside it, from 12–6 km corresponding to a density decrease of 0.1–0.8 g cm^{-3}. Theoretically, from the gravity models, mass deficiency can be calculated for partial melt interpretation, even though Isherwood did not attempt to do this. The preferred model consisted of a magma body with a radius of 6.9 km in which the density was less than in the surrounding rock by 0.5 g cm^{-3} (figure 18*b*). The residual gravity low near the steam production zone (where there is no evidence of surface volcanics) is interpreted as an extension of the magma chamber under Mt Hannah or a region of fractured rock filled with steam.

Detailed gravity surveys in the region of the Koryaksky and Avachinsky volcanoes in

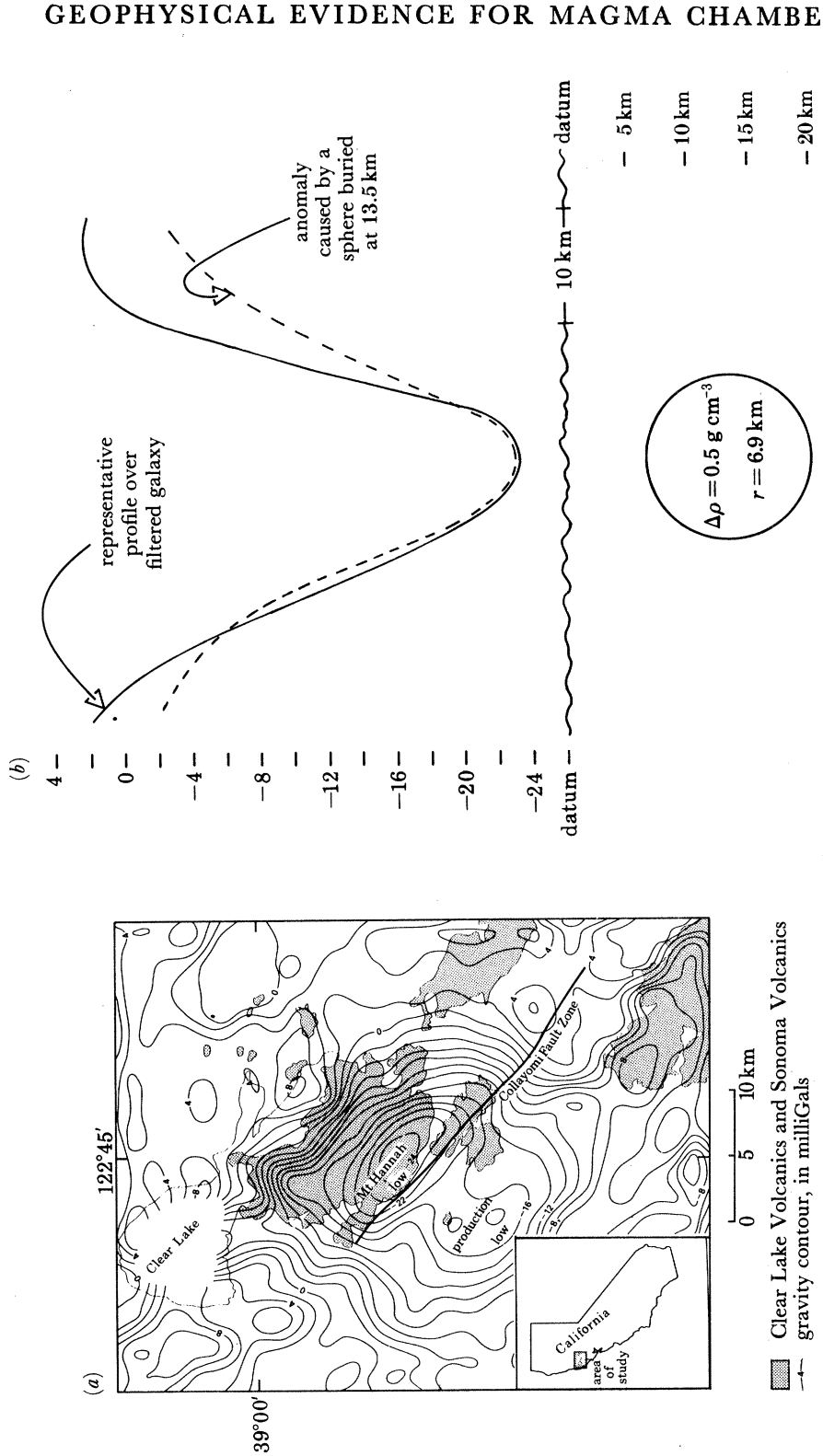

FIGURE 18. (*a*) Residual gravity map of the Geysers-Clear Lake volcanic field, California. Reduction density 2.67 g cm^{-3}. Contour interval 2 mGal. (*b*) Representative gravity profile (solid line) and computed curves for low-density sphere at 13.5 km depth (dashed line) (Isherwood 1976).

Kamchatka (Steinberg & Zubin 1964) showed that the volcanoes are located over a northwesterly band of positive anomalies interpreted as an intrusion of high density andesites and basalts. Within this anomaly was found a higher positive anomaly over the Avachinsky volcano which was interpreted as a ellipsoidal mass with a volume of about 50–100 km^3. Steinberg and Zubin interpret this body as a magma chamber but do not discuss the composition or the degree of melt in the chamber. In some of the other Kamchatka volcanoes gravity lows rather than highs seem to occur. These are interpreted as silicic magma chambers in which the density of melt is less than in the surrounding rock (Zubin 1979).

Numerous studies of regional gravity anomalies, both positive and negative are available. One such study, though not strictly related to detection of magma chambers, is worth mentioning here as it is related to an understanding of magma genesis. It is the detailed gravity modelling of the East African Rift (Fairhead 1976). In this region gravity highs occur and are interpreted as the replacement of the lithosphere by asthenospheric material beneath the rifts. The modelling of the gravity anomalies in Yellowstone National Park, U.S.A., is discussed in §5.5.1.

7. Magnetics

Magnetic field data have been used very little for exploration of magma chambers. Rocks lose their magnetization at the Curie point temperature and thus their ability to generate detectable magnetic fields. This property makes magnetic data potentially very useful in detecting the presence of hot rock and magma in the crust. The Curie point temperature for crustal rocks is about 560 °C and if the depth to the Curie isotherm can be determined, abnormally hot regions within the crust could be located.

Smith *et al.* (1974, 1977) and Bhattacharyya & Leu (1975) have determined the depth to the Curie isotherm in Yellowstone National Park, Wyoming, U.S.A. The principal features of the residual aeromagnetic map of Yellowstone are: a series of magnetic highs to the west of the caldera; a series of magnetic lows in the centre of the caldera; and a rapid rise in the magnetic field to the east and northeast of the caldera. Smith *et al.* (1974, 1977) first performed a pseudo-gravity transformation of the aeromagnetic data which gave essentially the thickness of a uniformly magnetized sheet of material that would give the observed residual magnetic anomaly pattern. The thickness of this material is proportional to the Curie isotherm depth. The magnetized layer was found to be about 10 km thick under the caldera and 30 km thick outside to the northeast and east, implying that the Curie isotherm was much shallower beneath the caldera than outside. Using a complex procedure involving the two-dimensional spectral estimates of the aeromagnetic data, Smith *et al.* determined the depth to the Curie isotherm to be 10 ± 3 km below sea level within the Yellowstone caldera. Based on this finding and other geophysical data, they proposed the presence of a large magma body under the Yellowstone caldera with its top at a depth of about 6 km below the surface (figure 19). This magma body was much larger laterally than that found under the Sour Creek resurgent dome with fan-shooting (see §4.2).

Bhattacharyya & Leu (1975) estimated the spatial variation of the depth to the Curie isotherm in the Yellowstone region. The Curie isotherm depths were found to be 7–8 km below the surface within the caldera and about 12 km to the northeast, northwest, and southwest of the caldera. The general trend of the contours was in a southwest–northeast direction, the same as the axis of the Eastern Snake River Plain–Yellowstone volcanic sub-province.

PHILOSOPHICAL TRANSACTIONS OF THE ROYAL SOCIETY A MATHEMATICAL, PHYSICAL & ENGINEERING SCIENCES

8. Electrical and electromagnetic methods

In these methods, resistivity of rocks is the principal property measured. In electrical methods, a direct current is introduced into the ground through electrodes driven into the ground and the electric field is measured by using two other mobile electrodes. Though the potential of electrical methods to study magma bodies is excellent as can be inferred from

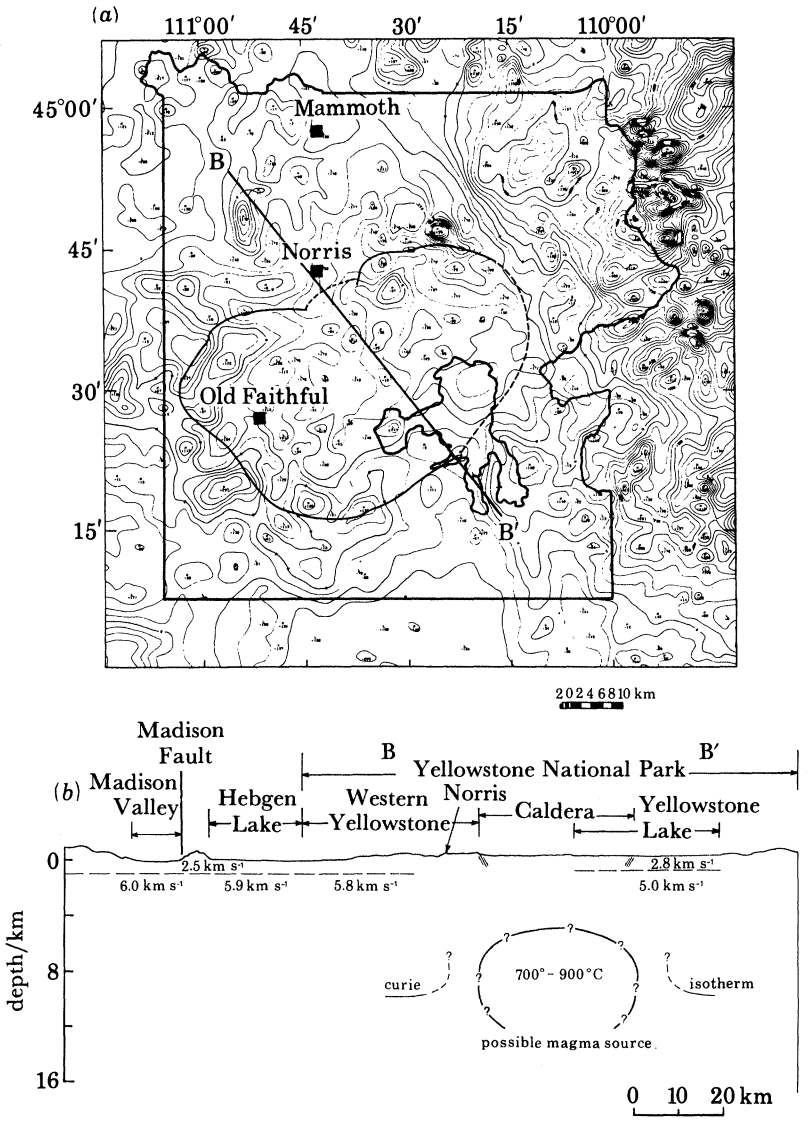

Figure 19. Residual magnetic map of Yellowstone National Park. The contour interval is 50 gammas. (*b*) Crustal model along profile B–B′ with magnetic field data. (Adapted from Smith *et al.* 1977.) Copyright American Geophysical Union.

the controlled experiments to study the Kilauea Iki lava lake (Hermance & Colp 1982), they are not yet widely used for the detection of magma bodies. In the electromagnetic method, variations in the Earth's magnetic and electric fields due to natural currents in the Earth are measured. The technique has been used extensively to study regional features, such as rift zones. Jiracek *et al.* (1979) and Hermance (1982) present extensive reviews on the use of the

electromagnetic technique to study the volcano-tectonic evolution of several of the world's major rift zones. The use of the technique in magma-related studies is best illustrated by summarizing a series of detailed studies in Iceland by Hermance & Grillot (1970, 1974), Hermance *et al.* (1976), and Thayer *et al.* (1981). The basic quantities measured are the orthogonal components of the electric and magnetic fields. By using the Fourier components

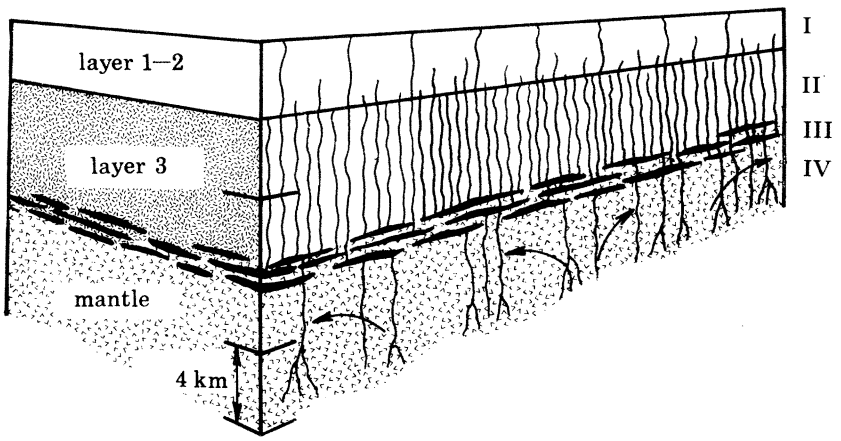

FIGURE 20. Schematic representation of a vertical cross section through the northern neovolcanic zone of Iceland, based on magnetotelluric data. The electrical zones are shown on the right, and the seismic zones are indicated on the left. See text for details (Thayer *et al.* 1981).

of these quantities, the apparent resistivity in ohm metres, at period T in seconds is computed. ρ is called the apparent resistivity because the essence of the magnetotelluric method is that resistivity is not constant with period because of the skin effect. The inversion from apparent to true resistivity is quite complex due to the inevitable presence of lateral inhomogeneities within the Earth. Once reasonable estimates of resistivity as a function of depth is estimated, good laboratory data are available for thermal and partial melt interpretations (Shankland & Waff 1977; Shankland *et al.* 1981). Electrical resistivity in rocks decreases as a function of temperature with a rapid decrease of one or two orders of magnitude occurring through melting.

In their magnetotelluric experiment in southwest Iceland, Hermance & Grillot (1970) found a low electrical resistivity of 10–20 Ωm at a depth of 15–20 km. This was interpreted as being due to the presence of rock at high temperatures in the range of 820–1120°, though the presence of partial melt was not definitely established. In a more sophisticated analysis of magnetotelluric data from additional areas in southwest Iceland, Hermance & Grillot (1974) found similar high temperatures (1000 ± 200 °C) in the crust–mantle interface. Thayer *et al.* (1981) conducted a detailed magnetotelluric survey in the Krafla region in the northern neovolcanic zone in Iceland. Using a Monte Carlo inversion technique to model the data, they identified a fairly large region with an anomalous conductive layer at the base of the crust. Figure 20 shows their comparison of the magnetotelluric model with the seismic and geologic model for the crust and mantle in the Krafla region of Iceland. Zone I is the region of hydrothermal alteration associated with seismic layers 1 and 2. Zone II, related to seismic layer 3, represents a region of basaltic intrusion and the electrical resistivity of 30 Ωm in this layer is explained as due to 2.5% partial melt. The most significant feature of the magnetotelluric model is Zone III with a resistivity of less than 10 Ωm in a layer of about 4 km thickness. This

is interpreted as a zone of magma accumulation in the crust–mantle boundary. The concentration of melt depends on the assumed thickness of the zone, varying from 15% for 4 km thickness to total melt for 200 m thickness. Zone IV is interpreted as a region through which magma transport takes place, probably in diapiric flows.

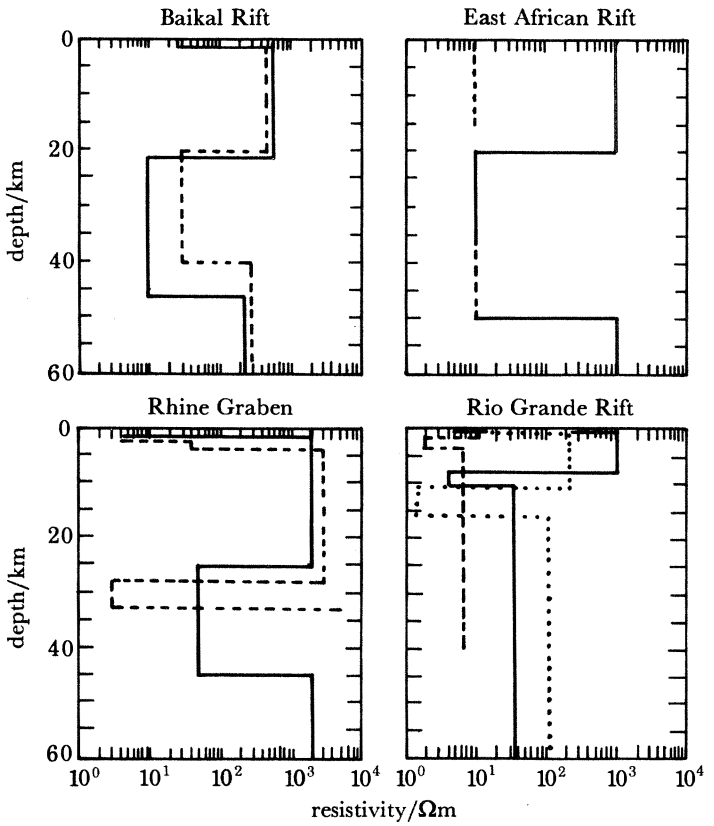

FIGURE 21. Geoelectric sections for the upper 60 km of the crust from various sources (Jiracek *et al.* 1979). The dashed and solid lines are intended to separate models by different investigators in the same region. Copyright American Geophysical Union.

Jiracek *et al.* (1979) and Hermance (1982) have reviewed the results of magnetotelluric surveys in several major rift zones of the Earth. In the Baikal rift in the Siberian platform in the U.S.S.R., an anomalous conductive zone of about 25 km thickness is found in the lower crust. Together with thermal modelling and other geophysical results, this zone is interpreted to be in a state of partial melting. A similar low resistivity zone seems to exist under the Rhine Graben at a depth of about 25 km, and under the Kenya rift in the East African Rift system at a depth of 20 km (figure 21). All these rifts also show lithospheric thinning and low upper mantle resistivities under the rift axes. The low resistivity and other geophysical data are interpreted as due to partial melting.

A magnetotelluric survey in the Socorro region of the Rio Grande Rift along a profile where reflections from the postulated magma chamber were seen in the seismic reflection data (see §4.5). Does not show any resistivity low which could be correlated with the postulated magma body at a depth of 19 km (Jiracek *et al.* 1979). Instead, a conductive horizon was seen at a depth of about 10 km (figure 21) which was interpreted as a volume of hydrous material, such

as amphibole. No explanation as to why the magma body itself was not seen as a conductivity anomaly was given. Hermance & Pederson (1980) report low-resistivity layers in two other areas of the Rio Grande Rift; near Santa Fe, New Mexico and El Paso, Texas. The conducting layer beneath El Paso is in the depth range of 21–28 km and in Santa Fe at a depth of 10–17 km.

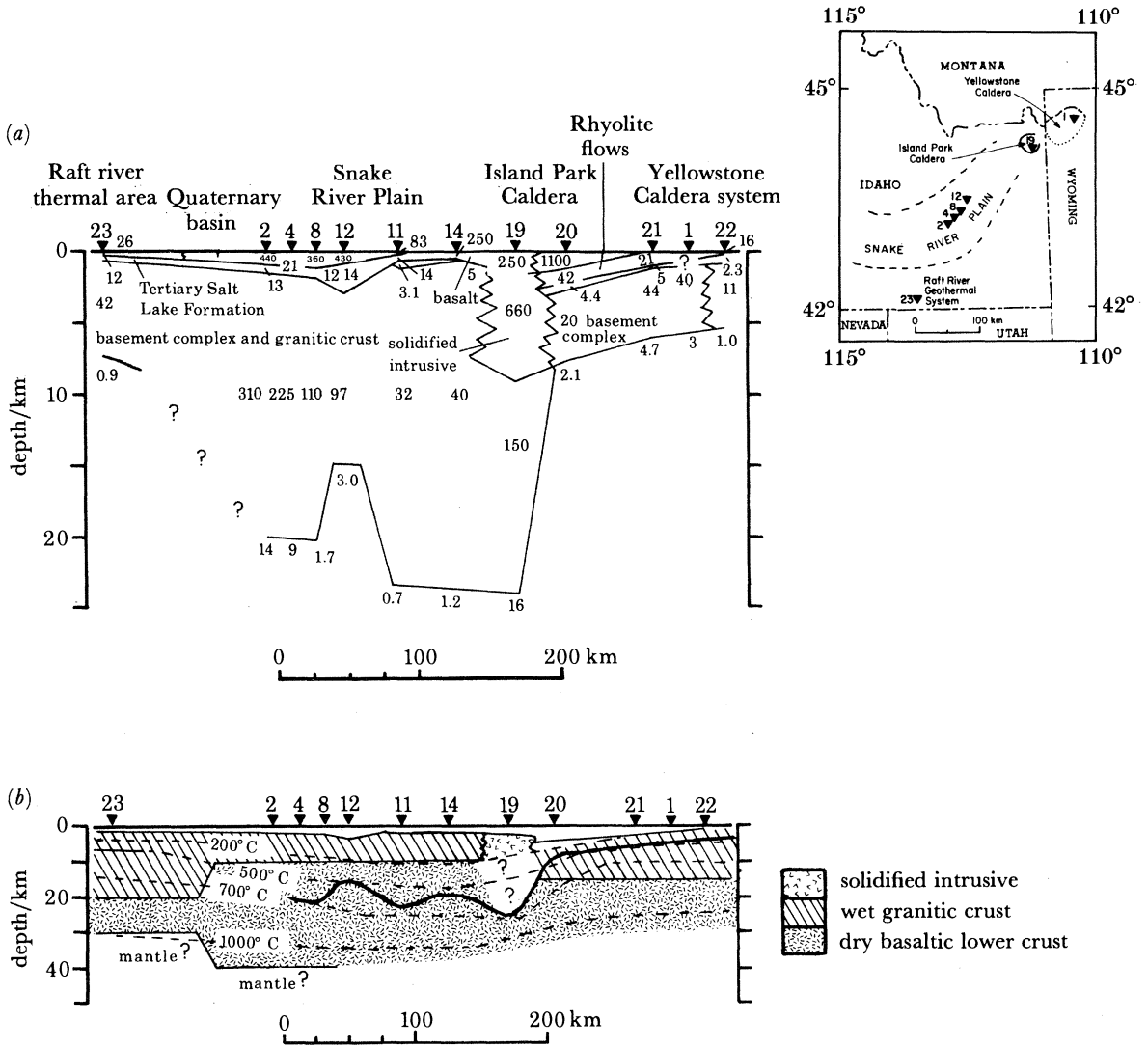

FIGURE 22. Geoelectric model for the Eastern Snake River Plain–Yellowstone region (*a*), and inferred thermal and geologic models from using seismic models as constraints (*b*). Triangles are magnetotelluric stations. Numbers in upper figure indicate resistivity in ohmmetres (Stanley *et al.* 1977). Copyright American Geophysical Union.

They suggest that these zones are contiguous with the magma sill suggested from other investigations (see §§4.5 and 5.3) near Socorro.

Detailed magnetotelluric soundings along a profile extending from the Raft River geothermal area in southern Idaho to Yellowstone National Park, Wyoming, reveal a highly anomalous crustal structure (Stanley *et al.* 1977). The geoelectrical cross section is shown in figure 22*a*. The most significant feature of the resistivity structure is the lowermost conductive layer that was detected, with resistivities ranging from 1 Ωm at the two ends of the profile at

about 7 km depth to 1–16 Ωm in the central region at a depth of 20 km. Stanley *et al.* considered various possible mechanisms, including partial melting, to explain the observed resistivity anomalies. To relate the observed anomalous resistivities to temperature structure they made a detailed analysis of the effect of water on resistivity of rocks as a function of temperature and pressure. Making a variety of assumptions and using available seismic models to constrain the type of rock along the profile, they have constructed the isothermal distribution as a function of depth and distance (figure 22*b*). If the model is assumed correct, the high temperatures at shallow depths under Yellowstone could cause partial melting of the granitic (rhyolitic) crust, whereas under the Eastern Snake River Plain, melting of the basaltic lower crust is not likely and magma can therefore be present only at sub-crustal depths. These findings are consistent with the teleseismic studies in the Eastern Snake River Plain and Yellowstone (see §§5.5.1 and 5.5.2).

9. Summary

Geophysical tools commonly used in resource exploration and earth-structure studies are also suited for the detection of magma chambers. Active seismic techniques, with controlled sources, and passive seismic techniques, with local and regional earthquakes and teleseisms, can be used to detect the drastic changes in velocity and attenuation that occur at the onset of melting of rocks and to delineate in three dimensions the shape of the partly melted zone. Similarly, decreases in density and electrical resistivity in rocks during melting, can be detected. Seismic refraction and reflection are not yet used extensively in magma chamber studies. In a study, in the Yellowstone region, seismic delays occurring in a fan-shooting configuration and time-term modelling show the presence of an intense molten zone in the upper crust. Deep seismic sounding (a combination of seismic refraction and reflection) and modelling amplitude and velocity changes of diffracted seismic waves from explosions and earthquakes, have enabled mapping of small and large magma chambers beneath many volcanoes in Kamchatka, U.S.S.R. Teleseismic P-wave residuals have been used to model low-velocity bodies, interpreted as magma chambers, in several Quaternary volcanic centres in the U.S.A. The results show that magma chambers with volumes of a few hundred to a few thousand cubic kilometres volume seem to be confined to regions of silicic volcanism. Many of the magma bodies seem to have upper-mantle roots implying that they are not isolated pockets of partial melt, but may be deriving their magma supplies from deeper parental sources. Medium or large crustal magma chambers are absent in the andesitic volcanoes of western United States and the basaltic Kilauea volcano, Hawaii. However, regional velocity models of the Oregon Cascades and Hawaii show evidence for the presence of magma reservoirs in the upper mantle. The transport of magma to the upper crust in these regions probably occurs rapidly through narrow conduits, with transient storage occurring in small chambers of a few cubic kilometres volume.

Very little use has been made of the gravity and magnetic maps to model magma chambers. The number of available case histories, though few, indicate that these data can be very useful to give constraints on the density and temperature in magma chambers. Seismic, gravity, and electromagnetic techniques have been used to model regional structure in several rift zones of the world. Together the data indicate lithospheric thinning under the rifts with possible sub-crustal storage of magma and diapiric intrusions into the crust.

The current status of the use of geophysical techniques in magma chamber studies can be summarized as follows. Though powerful experimental methods for data collection and

PHILOSOPHICAL TRANSACTIONS OF THE ROYAL SOCIETY A MATHEMATICAL, PHYSICAL & ENGINEERING SCIENCES

mathematical and computational techniques for modelling are available, the two dozen or so available case histories seem to represent isolated, technique-oriented studies. Only in a few regions, such as Kamchatka, U.S.S.R., and Yellowstone and Socorro, U.S.A., are data from multiple geophysical techniques becoming available. Several studies in different tectonic and volcanic environments, which use a suite of geophysical experiments capable of measuring different physical properties of rocks and having a wide range of resolutions, are needed to understand the problems of magma generation, migration, and storage.

Many figures, data and results presented in this paper are from several different publications. I am indebted to the authors and publishers for permitting their use. I am very grateful to some of the authors who supplied photo prints of figures. Tim Hitchcock's help in preparing and organizing the figures was invaluable. Dr F. W. Klein, Dr W. D. Mooney, and Dr R. S. J. Sparks reviewed the manuscript and made useful suggestions.

References

Aki, K., Christoffersson, A. & Husebye, E. S. 1976 *Bull. seism. Soc. Am.* **66**, 501–524.
Aki, K., Christoffersson, A. & Husebye, E. S. 1977 *J. geophys. Res.* **82**, 277–296.
Armstrong, R. L., Leeman, W. P. & Malde, H. E. 1975 *Am. J. Sci.* **275**, 225–251.
Balesta, S. T. & Farberov, A. I. 1968 *Bull. volcan.* XXXII, 395–399.
Balesta, S. T., Kargopoltsev, A. A. & Grigoryan, G. B. 1978 *Bull. volcan.* XXXXI, 473–479.
Bhattacharyya, B. K. & Leu, L. 1975 *J. geophys. Res.* **80**, 4461–4465.
Brocher, T. M. 1981 *J. geophys. Res.* **86**, 9420–9432.
Brown, L. D., Chapin, C. E., Sanford, A. R., Kaufman, S. & Oliver, J. 1980 *J. geophys. Res.* **85**, 4773–4800.
Daniel, R. G. & Boore, D. M. 1982 *J. geophys. Res.* **87**, 2731–2744.
Duffield, W. A., Christiansen, R. L., Koyanagi, R. Y. & Peterson, D. W. 1982 *J. Volcan. geotherm. Res.* **13**, 273–307.
Edmond, J. M. 1983 *Rev. Geophys. Space Phys.* **21**, 1384–1386.
Einarsson, P. 1978 *Bull. volcan.* XXXXI, 187–195.
Ellsworth, W. L. & Koyanagi, R. Y. 1977 *J. geophys. Res.* **82**, 5379–5394.
Endo, E. T., Malone, S. D., Noson, L. L. & Weaver, C. S. 1981 In *The 1980 Eruptions of Mount St Helens, Washington, U.S. Geological Survey Professional Paper 1250* (ed. P. W. Lipman & D. R. Mullineaux), pp. 93–107. Washington, D.C.: U.S. Government Printing Office.
Evans, J. R. 1982 *J. geophys. Res.* **87**, 2654–2670.
Evoy, J. A. 1978 M.S. thesis, University of Utah, Salt Lake City, Utah.
Fairhead, J. D. 1976 *Tectonophysics* **30**, 269–298.
Farberov, A. I. & Gorelchik, V. I. 1971 *Bull. volcan.* XXXV, 212–224.
Farberov, A. I., Gorelchik, V. I. & Zubkov, S. I. 1973 *Bull. volcan.* XXXVII, 122–133.
Farberov, A. I., Gorelchik, V. I. & Zubkov, S. I. 1979 *Bull. volcan.* XXXXII, 75–89.
Fedotov, S. A. 1973 In *The Western Pacific: Island Arcs, Marginal Seas, Geochemistry* (ed. P. J. Coleman), pp. 247–254. Nedlands: The University of Western Australia Press.
Firstov, P. P. & Shirokov, V. A. 1971 *Bull. volcan.* XXXV, 164–172.
Fowler, C. M. R. 1976 *Geophys. Jl R. astr. Soc.* **47**, 459–491.
Fowler, C. M. R. 1978 *Geophys. Jl R. astr. Soc.* **54**, 167–183.
Fuis, G. S., Mooney, W. D., Healy, J. H., McMechan, G. A. & Lutter, W. J. 1982 In *The Imperial Valley, California, Earthquake of October 15, 1979, U.S. Geological Survey Professional Paper 1254*, pp. 25–49. Washington, D.C.: U.S. Government Printing Office.
Gorshkov, G. S. 1958 *Bull. volcan.* XIX, 103–113.
Hale, L. D., Morton, C. J. & Sleep, N. H. 1982 *J. geophys. Res.* **87**, 7707–7717.
Hermance, J. F. 1982 In *Continental and oceanic rifts* (ed. G. Palmason), pp. 169–192. Washington, D.C.: American Geophysical Union.
Hermance, J. F. & Colp, J. L. 1982 *J. Volcan. geotherm. Res.* **13**, 13–61.
Hermance, J. F. & Grillot, L. R. 1970 *J. geophys. Res.* **75**, 6582–6591.
Hermance, J. F. & Grillot, L. R. 1974 *Physics of the Earth and Planet. Int.* **8**, 1–12.
Hermance, J. F. & Pederson, J. 1980 *J. geophys. Res.* **85**, 3899–3912.

PHILOSOPHICAL TRANSACTIONS OF THE ROYAL SOCIETY A MATHEMATICAL, PHYSICAL & ENGINEERING SCIENCES

Hermance, J. F., Thayer, R. F. & Björnsson, A. 1976 In *Proceedings of the Second U.N. Symposium on the Development and Use of Geothermal Resources*, vol. 2, pp. 1037–1048. Washington, D.C.: U.S. Government Printing Office.
Herron, T. J., Ludwig, W. J., Stoffa, P. L., Kan, T. K. & Buhl, P. 1978 *J. geophys. Res.* **83**, 798–804.
Hill, D. P. 1969 *Bull. seism. Soc. Am.* **59**, 101–130.
Hill, D. P. 1976 *J. geophys. Res.* **81**, 745–753.
Isherwood, W. F. 1976 In *Proceedings of the Second U.N. Symposium on the Development and Use of Geothermal Resources*, vol. 2, pp. 1065–1073. Washington, D.C.: U.S. Government Printing Office.
Iyer, H. M. 1975 *Nature, Lond.* **253**, 425–427.
Iyer, H. M. 1983 *Tectonophysics* (In the press.)
Iyer, H. M., Evans, J. R., Zandt, G., Stewart, R. M., Coakley, J. M. & Roloff, J. N. 1981 *Bull. geol. Soc. Am.* **92**, part 1, 792–798, part II (Microfiche edition), 1471–1646.
Iyer, H. M., Oppenheimer, D. H., Hitchcock, T., Roloff, J. N. & Coakley, J. M. 1981 In *Research in The Geysers-Clear Lake Geothermal Area, California, U.S. Geological Survey Professional Paper* 1141 (ed. R. J. McLaughlin & J. M. Donnelly-Nolan), pp. 97–116. Washington, D.C.: U.S. Government Printing Office.
Iyer, H. M., Rite, A. & Green, S. M. 1982 In *Technical Programs Abstracts and Biographies, Society of Exploration Geophysicists* (*Fifty-second Annual International Meeting and Exposition*), pp. 479–482. Oklahoma: Tulsa.
Iyer, H. M. & Stewart, R. M. 1977 In *Proceedings of the American Geophysical Union Chapman Conference on Partial Melting in the Upper Mantle* (ed. H. J. B. Dick), pp. 281–299. Portland, Oregon: Oregon Department of Geology and Mineral Industries.
Jiracek, G. R., Ander, M. E. & Holcombe, H. T. 1979 In *Rio Grande Rift: Tectonics and Magmatism* (ed. R. E. Riecker), pp. 209–222. Washington, D.C.: American Geophysical Union.
Koyanagi, R. Y., Endo, E. T. & Ebisu, J. S. 1975 *Geophys. Res. Lett.* **2**, 405–408.
Koyanagi, R. Y., Unger, J. D., Endo, E. T. & Okamura, A. T. 1976 *Bull. volcan.* XXXIX, 621–631.
Kubota, S. & Berg, E. 1967 *Bull. volcan.* XXXI, 175–214.
Latter, J. H. 1981 *J. Volcan. geotherm. Res.* **10**, 125–156.
Lehman, J. A., Smith, R. B., Schilly, M. M. & Braile, L. W. 1982 *J. geophys. Res.* **87**, 2713–2730.
Macdonald, K. C. 1983 *Rev. Geophys. Space Phys.* **21**, 1441–1454.
Manghanani, M. H., Rai, C. S., Katahara, K. W. & Olhoeft, G. R. 1981 In *Anelasticity of the Earth, geodynamic series*, vol. 4 (ed. F. D. Stacey, A. Paterson & A. Nicholas), pp. 118–122. Washington, D.C.: American Geophysical Union.
Matumoto, T. 1971 *Bull. geol. Soc. Am.* **82**, 2905–2920.
Mavko, G. M. 1980 *J. geophys. Res.* **85**, 5173–5189.
Murase, T. & McBirney, A. B. 1973 *Bull. geol. Soc. Am.* **84**, 3563–3592.
Nisbet, E. G. & Fowler, C. M. R. 1978 *Geophys. Jl R. astr. Soc.* **54**, 631–660.
O'Connell, R. J. & Budiansky, B. 1974 *J. geophys. Res.* **79**, 5412–5426.
Okada, Hm., Watanabe, H., Yamashita, H. & Yokoyama, I. 1981 *J. Volcan. geotherm. Res.* **9**, 311–336.
Orcutt, J. A., Kennett, B. L. N. & Dorman, L. M. 1976 *Geophys. Jl R. astr. Soc.* **45**, 305–320.
Oppenheimer, D. H. & Herkenhoff, K. E. 1981 *J. geophys. Res.* **86**, 6057–6065.
Piermattei, R. & Adams, W. M. 1973 *Annali de Geofisica* XXVI, 525–559.
Reasenberg, P., Ellsworth, W. & Walter, A. 1980 *J. geophys. Res.* **85**, 2477–2483.
Rinehart, E. J., Sanford, A. R. & Ward, R. M. 1979 In *Rio Grande Rift: tectonics and magmatism* (ed. R. E. Riecker), pp. 237–251. Washington, D.C.: American Geophysical Union.
Robinson, R. & Iyer, H. M. 1981 *Geophysics* **46**, 1456–1466.
Rosendahl, B. R. 1976 *J. geophys. Res.* **81**, 5305–5314.
Rosendahl, B. R., Raitt, R. W., Dorman, L. M., Bibee, L. D., Hussong, D. M. & Sutton, G. H. 1976 *J. geophys. Res.* **81**, 5294–5304.
Ryall, F. & Ryall, A. 1981 *Geophys. Res. Lett.* **8**, 557–560.
Ryan, M. P., Koyanagi, R. Y. & Fiske, R. S. 1981 *J. geophys. Res.* **86**, 7111–7129.
Sanford, A. R., Alptekin, O. & Toppozada, T. R. 1973 *Bull. seism. Soc. Am.* **63**, 2021–2034.
Sanford, A. R. & Einarsson, P. 1982 In *Continental and oceanic rifts* (ed. A. Pálmason), pp. 147–1682. Washington, D.C.: American Geophysical Union.
Sanford, A. R. & Long, L. T. 1965 *Bull. seism. Soc. Am.* **55**, 579–586.
Sanford, A. R., Mott, Jr, R. P., Shuleski, P. J., Rinehart, E. J., Caravella, F. J., Ward, R. M. & Wallace, T. C. 1977 In *The Earth's crust* (ed. J. G. Heacock), pp. 385–403. Washington, D.C.: American Geophysical Union.
Savage, J. C. & Clark, M. M. 1982 *Science, Wash.* **217**, 531–533.
Savino, J. M., Rodi, W. L. & Jordan, T. H. 1979 *Geothermal Resources Council Transactions* **3**, 625–628.
Schilly, M. M., Smith, R. B., Braile, L. W. & Ansorge, J. 1982 *J. geophys. Res.* **87**, 2692–2704.
Shankland, T. J., O'Connel, R. J. & Waff, H. S. 1981 *Rev. Geophys. Space Phys.* **19**, 391–406.
Shankland, T. J. & Waff, H. S. 1977 *J. geophys. Res.* **82**, 5409–5417.
Sharp, A. D. L., Davis, P. M. & Gray, F. 1980 *Nature, Lond.* **287**, 587–591.

PHILOSOPHICAL TRANSACTIONS OF THE ROYAL SOCIETY A MATHEMATICAL, PHYSICAL & ENGINEERING SCIENCES

Smith, R. B., Schilly, M. M., Braile, L. W., Ansorge, J., Lehman, J. L., Baker, M. R., Prodehl, C., Healy, J. H., Mueller, S. & Greensfelder, R. W. 1982 *J. geophys. Res.* **87**, 2583–2596.
Smith, R. B., Shuey, A. T., Friedline, R. O., Otis, R. M. & Alley, L. B. 1974 *Geology* **2**, 451–455.
Smith, R. B., Shuey, R. T., Pelton, J. R. & Bailey, J. P. 1977 *J. geophys. Res.* **82**, 3665–3676.
Stanley, W. D., Boehl, J. E., Bostick, F. X. & Smith, H. W. 1977 *J. geophys. Res.* **82**, 2501–2514.
Stauber, D. A. 1982 *J. geophys. Res.* **87**, 5451–5459.
Steeples, D. W. & Iyer, H. M. 1976 *J. geophys. Res.* **81**, 849–860.
Steinburg, G. S. & Zubin, M. I. 1964 *Tectonophysics* **1**, 357–363.
Thayer, R. E., Björnsson, A., Alvarez, L. & Hermance, J. F. 1981 *Geophys. Jl R. astr. Soc.* **65**, 423–442.
Utnasin, V. K., Abdurakhmanov, A. I., Anosov, G. I., Budyansky, Yu. A., Fedorchenka, V. I., Markhinin, Ye. K. & Balesta, S. T. 1976 In *Volcanoes and tectosphere* (ed. H. Aoki & S. Iizuka), pp. 123–137. Tokyo, Japan: *Tokai University Press.*
Ward, R. M., Schule, J. W. & Sanford, A. R. 1981 *Geophys. Res. Lett.* **8**, 553–556.
Ward, R. W. & Young, C. 1980 *J. geophys. Res.* **85**, 5227–5236.
Weaver, C. S., Green, S. M. & Iyer, H. M. 1982 *J. geophys. Res.* **87**, 2782–2792.
Young, C. & Ward, R. W. 1980 *J. geophys. Res.* **85**, 2459–2470.
Young, C. & Ward, R. M. 1981 In *Research in The Geysers-Clear Lake Geothermal Area, California* (*U.S. Geological Survey Professional Paper* 1141) (ed. R. J. McLaughlin & J. M. Donnelly-Nolan), pp. 149–160. Washington, D.C.: U.S. Government Printing Office.
Zubin, M. I. 1979 *Bull. volcan.* XXXXII, 89–93.
Zucca, J. J. & Hill, D. P. 1980 *Bull. seism. Soc. Am.* **70**, 1149–1159.
Zucca, J. J., Hill, D. P. & Kovach, R. L. 1982 *Bull. seism. Soc. Am.* **72**, 1535–1550.

PHILOSOPHICAL TRANSACTIONS OF THE ROYAL SOCIETY A MATHEMATICAL, PHYSICAL & ENGINEERING SCIENCES

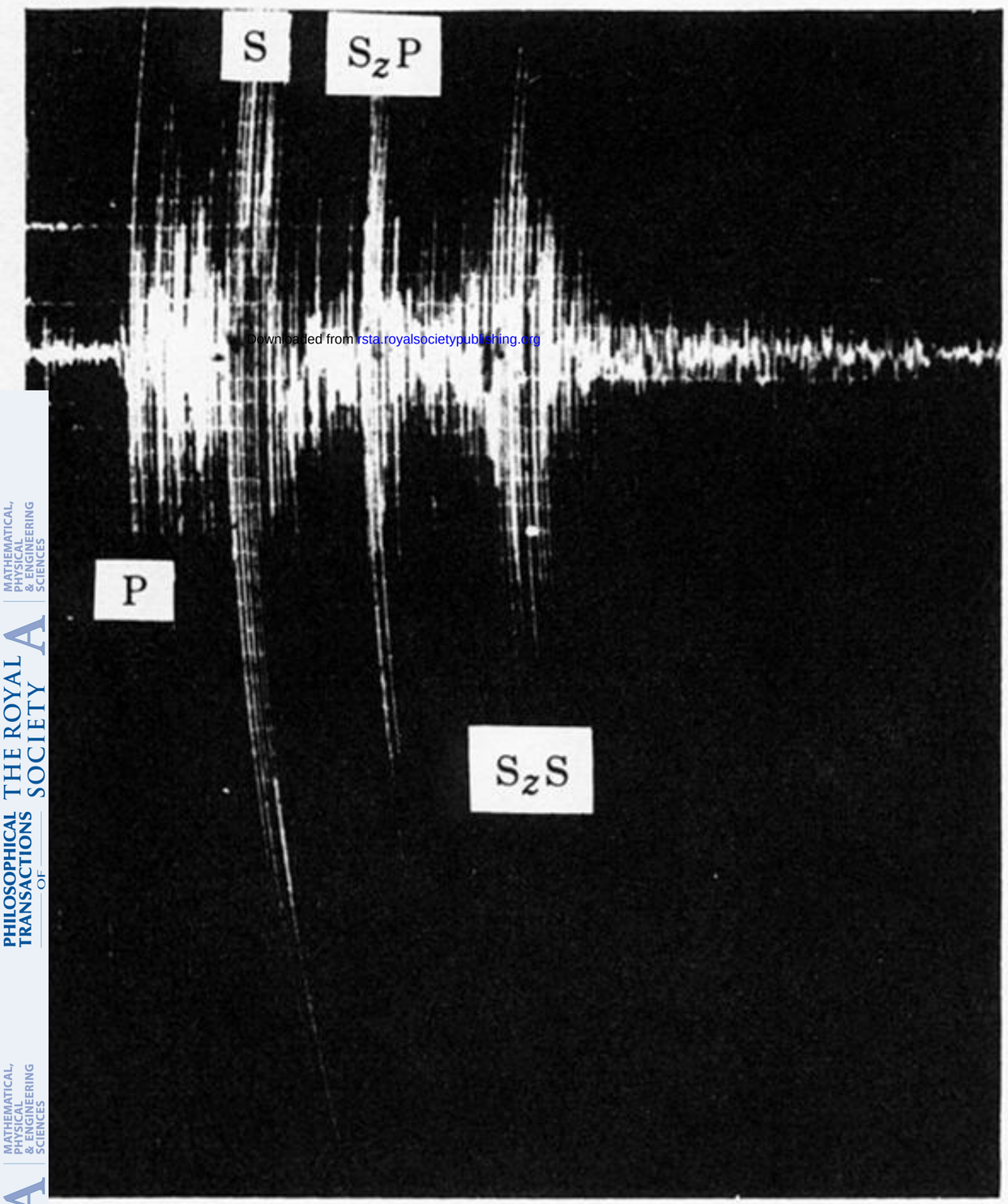

FIGURE 12. (*a*) A micro-earthquake seismogram in the Socorro region, New Mexico. P- and S-phases and sharp reflected phases S_zP and S_zS are seen. (*b*) A map of well located reflection points. Boundaries of the inferred sill-like magma body are shown by solid lines where well constrained and dashed lines were poorly constrained. Triangles show seismic stations. Also shown are the Vibroseis reflection profiles (Rinehart *et al.* 1979). Copyright American Geophysical Union.